CRC Project No. AV-16-11

STUDIES OF SCANNING BROOKFIELD VISCOMETRY AS A REPLACEMENT FOR FREEZING POINT IN AVIATION FUEL SPECIFICATIONS

Final Report

October 2013

COORDINATING RESEARCH COUNCIL, INC.
5755 NORTH POINT PARKWAY·SUITE 265·ALPHARETTA, GA 30022

The Coordinating Research Council, Inc. (CRC) is a non-profit corporation supported by the petroleum and automotive equipment industries. CRC operates through research committees made up of technical experts from industry and government who voluntarily participate. The four main areas of research within CRC are: air pollution (atmospheric and engineering studies); aviation fuels, lubricants, and equipment performance; heavy-duty vehicle fuels, lubricants, and equipment performance (e.g., diesel trucks); and light-duty vehicle fuels, lubricants, and equipment performance (e.g., passenger cars). CRC's function is to provide the mechanism for joint research conducted by the two industries that will help in determining an optimum combination of petroleum products and mobility equipment. CRC's work is limited to research that is mutually beneficial to the two industries involved. Final reports and data are made available to the public.

UDRI
UNIVERSITY of DAYTON RESEARCH INSTITUTE

UDR-TR-2013-100

STUDIES OF SCANNING BROOKFIELD VISCOMETRY AS A REPLACEMENT FOR FREEZING POINT IN AVIATION FUEL SPECIFICATIONS

Submitted to:

Coordinating Research Council, Inc.
5755 North Point Parkway, Suite 265
Alpharetta, GA 30022

Submitted by:

S. Zabarnick, Z.J. West, L.M. Shafer, and R. Cook
University of Dayton Research Institute
300 College Park
Dayton OH 45469-0140

OCTOBER 2013

Table of Contents

Executive Summary

The CRC Aviation Committee funded this study to evaluate viscosity methods which relate to fuel flow and pumpability as potential replacements for the current freezing point requirement in jet fuel specifications. To address this goal, the current work is an experimental study utilizing Scanning Brookfield Viscometry (SBV) (ASTM D5133) and Freezing Point measurements (ASTM D5972) over a range of fuel samples and temperatures. These data have been used to select viscosity parameters which relate to fuel pumpability and flowability. Initially, the use of the viscosity "knee temperature" upon cooling was studied. The data were used to estimate a viscosity equivalent to the current freezing point specification limit for jet fuel. Chemical analyses of fuel n-alkane distributions were performed to determine how these distributions affected freezing point, viscosity and their specifications.

This study demonstrated that the "viscosity knee" temperature measurement correlates very well with measured freezing point and exhibits excellent repeatability. But since the "viscosity knee" temperature correlates so closely with freezing point, it is unlikely that this new parameter will provide any additional benefit in correlating more closely to fuel flowability and pumpability. This study also provided viscosity limit measurements and analyses yielding viscosity data and maximum limits that can be used to construct a viscosity "equivalent limit" for current specification fuels. The calculated maximum limits at various low temperatures imply that fuel viscosities are significantly higher than expected when compared to engine OEM operability limits.

Some of the current freezing point measurement methods (e.g., ASTM D5972) have been shown to be able to detect contamination from small amounts of higher molecular weight petroleum products, such as diesel fuels and heating oils. Viscosity is a parameter that tends to be more sensitive to the fuel constituents that are in higher concentration, rather than low concentration contaminants. Thus a viscosity specification is less likely to successfully detect the presence of such contaminants. Thus it is desirable to retain both viscosity and freezing point specifications for jet fuels. One alternative is to eliminate the freezing point specification, but replace it with the SBV knee temperature. The results reported here show excellent correlation between these two methods. Thus the scanning Brookfield viscometer viscosity and viscosity knee temperature results could be used to replace the capillary viscometer and freezing point method, respectively. A significant negative aspect of the SBV measurements is the long test duration, although faster scanning times may provide equivalent results.

Introduction

In 2008 the IATA Technical Fuel Group reported in their study of "Fuel Freezing Point Harmonisation" (1) that "it is a generally accepted fact that the FP test is not an effective method for predicting fuel flow behavior in the aircraft at low temperatures. The industry needs to embrace the concept of fuel flow and pumpability and seek better test methods to predict fuel flow in these conditions." This conclusion led to a 2009 CRC study entitled "Develop an Aviation Fuel Cold Flowability Test to Replace Freezing Point Measurement." The CRC study concluded: "at low temperatures down to below the freezing point to approximately the cloud point of the fuel, a flow method such as viscosity, more accurately predicts pumpability from an aircraft fuel tank than freezing point."

As a result of these previous studies, the CRC Aviation Committee has funded the current study to evaluate viscosity methods which relate to fuel flowability and pumpability to replace the current freezing point requirement in jet fuel specifications.

The program objectives are to:

1. Determine a 'viscosity equivalent' of the current freezing point specification limits.
2. Quantify the possible changes in fuel chemistry of jet fuel if a viscosity specification limit replaces freezing point.
3. Note that the buy-in from the OEM's is essential to agree how such a test compares with their needs to set a pass/fail test.

To address these goals, the current program included an experimental program utilizing Scanning Brookfield Viscometry (SBV) (ASTM D5133) and Freezing Point measurements (ASTM D5972) over a range of fuel samples. These data have been used to select viscosity parameters which relate to fuel pumpability and flowability. The use of the viscosity "knee temperature" upon cooling was studied. These data were used to estimate a viscosity equivalent to the current freezing point specification limit for jet fuel. Chemical analyses of fuel n-alkane distributions were performed to determine how these distributions affect freezing point, viscosity and their specifications.

Background and Issues

As fuel is cooled, the liquid viscosity begins to increase. With further cooling to sufficiently low temperatures, fuel species begin to crystallize. These crystals begin to form a matrix which entraps liquid fuel components, ultimately completely inhibiting fuel flow. Differential scanning calorimetry (DSC) can be used to elucidate these phase change phenomena by monitoring the flow of energy while heating or cooling a fuel sample. For example, Figure 1 shows DSC results for a Jet A fuel (sample F3219) that was cooled to -65 °C at a rate of -1 °C/min, then heated at 1°C/min to -45 °C. The large exothermic peak near -55 °C, obtained upon cooling, signifies the rapid formation of wax crystals. However, the broad, shallow endothermic peak, centered near -50°C, obtained during heating shows that the melting of these wax crystals takes place over a wider temperature range. These results show that the liquid-solid phase transition differs upon cooling and heating. These effects need to be considered when developing methods and

specifications regarding the freezing and low temperature flowability characteristics of jet fuels. For example, the jet fuel freezing point specification is actually the temperature where the last observable wax crystal melts upon heating (i.e., a chemist's melting point), which is a conservative measure of fuel freezing as most fuels will not begin to crystallize until a few degrees below the freezing point.

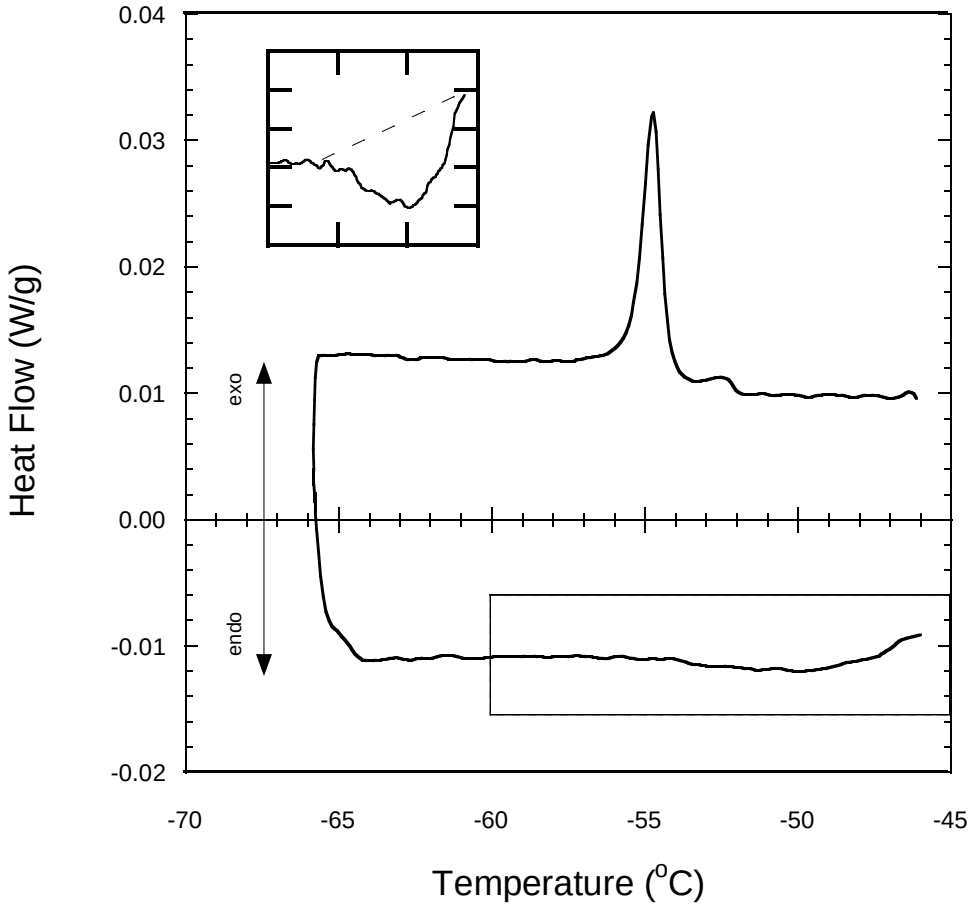

Figure 1. DSC results for a Jet A fuel (F3219) with a cooling and heating rate of 1 °C/min; expanded inset of boxed portion shows broad melting endotherm.

Cloud point (ASTM D5773) and pour point temperatures (ASTM D5949) are additional properties commonly measured for diesel fuels, but not normally used for jet fuels. Here we utilize these parameters to illustrate the processes which occur upon fuel crystallization. The cloud point is the temperature when the first observable solid wax crystal precipitates out of solution upon cooling, while the pour point is the lowest temperature at which fuel is able to flow upon cooling. Figure 2 shows DSC exotherms (with a cooling rate of -1 °C/min) for three jet fuel samples. The measured cloud, pour, and freezing points are shown for each fuel with circle, triangle, and square markers, respectively. The figure shows that the cloud and pour points bracket the liquid-solid phase transition (exothermic peak) with the cloud point occurring near the onset of the exotherm and the pour point occurring at the end of the exotherm, when crystallization is complete. The measured freezing point temperature is a few degrees warmer

than the cloud point and occurs upon heating at the end of the endothermic peak (not shown in Figure 2). Since the freezing point is measured upon heating and is a static (non-flowing) measurement, there is some question as to how well it represents fuel flowability characteristics during cooling in aircraft tanks and fuel feedlines.

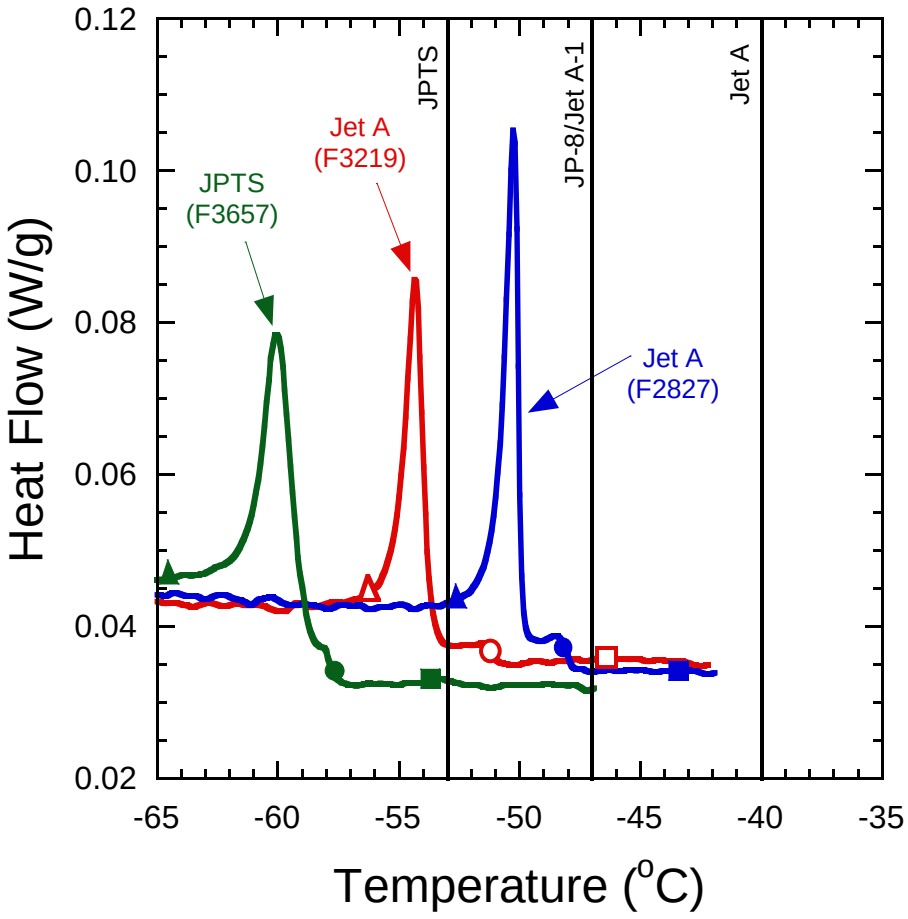

Figure 2. DSC exotherms of three different jet fuels for a cooling rate of 1 °C/min; triangle markers = pour point (ASTM D5949), circle markers = cloud point (ASTM D5773), and square markers = freezing point (ASTM D5972) for each fuel; maximum freezing point temperatures shown for select jet fuel specifications.

Current jet fuel specifications utilize a freezing point measurement, along with a kinematic viscosity measurement at a single temperature, to specify the low temperature properties of the fuel. While the specifications have generally allowed safe operation of aircraft worldwide, there is a view in the industry that these test methods do not sufficiently predict the low temperature performance of jet fuel during actual aircraft operations on long duration, high altitude flight (1). Recently, CRC funded a study to explore various improved methods to assess fuel low temperature properties (2). UDRI supplied much of the data used by the author in the analysis. The study provided the following recommendations:

1. Development and assessment of a suitable low temperature scanning viscometer for jet fuel specification use. The most suitable method would have good precision and be an accurate predictor of low temperature pumpability. A method based on D5133 appears to be suitable but other methods such as ones based on D445 and D7042 may also be suitable.
2. Investigate and identify a 'viscosity equivalent' limit that may be used for specification purposes.
3. Investigation and quantification of the likely small chemistry change of fuel if a viscosity test replaces freezing point.
4. Engage with OEM's to evaluate their support for replacing freezing point with viscosity and to find out if further rig or aircraft testing would be necessary.

UDRI has performed extensive studies of fuel low temperature flowability in research funded by the U.S. Air Force Research Laboratory and the U.S. Federal Aviation Administration. These studies, performed at the Air Force Research Laboratory facilities at Wright-Patterson AFB, OH, are documented in a series of journal publications, technical reports, and conference proceedings (3-27). In addition, a great deal of unpublished data was generated that has been employed in the current CRC study. The published work has included development and testing of a low temperature flow improving additive, JP-8+100LT, for use in the USAF U-2 and Global Hawk aircraft; studies of jet fuel crystallization via low temperature optical microscopy and DSC; flow visualization during fuel freezing and development of a computational model of the process; studies of fuel blends and low temperature flow improving additives via DSC; studies of improving low temperature jet fuel properties via urea treatment; effect of aircraft operation near the measured fuel freezing point on fuel flowability and pumpability; prediction of jet fuel freezing point temperatures using a thermodynamic model; and studies of jet fuel freezing using Scanning Brookfield Viscometry.

Scanning Brookfield Viscosity

The Scanning Brookfield Viscosity (SBV) technique (ASTM D5133) is a method and instrument developed in 1980 to resolve the cause of low temperature pumping failure of engine oils. For low viscosity fuels research, a special viscometer head is connected to a matched rotor-stator cell which is suspended in a controlled temperature bath. The fluid of interest is measured into the stator, which is held by an alignment fixture attached to the viscometer head. The rotor (spindle) is then suspended from the viscometer drive shaft within the stator. The stator and assembly are immersed in the bath which has been brought to the initial temperature, the viscometer head is turned on to the desired rotor speed and the bath ramping rate initiated. A cascade cooling system controls the bath temperatures between +30 and -75°C. A typical cooling profile involves quick cooling the sample to -20°C, holding for 2 minutes for equilibration, then cooling at -5°C per hour to the final temperature. If a warming curve is desired, operation is continued while the bath is gradually warmed to -20°C. The rotation rate of the spindle can be varied to investigate whether the fuel behaves as a Newtonian fluid, which may be useful in detection of fuel contaminants, additives, or adulterants. The complete system (Scanning Brookfield Plus Two Viscometer) was obtained from the Tannas Co.

Figure 3 shows scanning Brookfield viscometer results for a series of nine Jet A fuels over the temperature range -40°C to the temperature at the 200 cP limit of the viscometer measurement (using a 12 rpm rotation rate). The fuels exhibit freezing points over the range -44 to -55°C. While the fuels exhibit varied behavior vs. temperature, there are obvious commonalities. The fuels all have similar viscosities at the highest temperatures employed, near -40°C, where all the fuels are liquids. They all display a gradual increase in viscosity with decreasing temperature and a sudden increase in viscosity three or four degrees below their freezing point. Low temperature microscopy reveals that crystal formation begins at the temperature of this sudden viscosity rise (14).

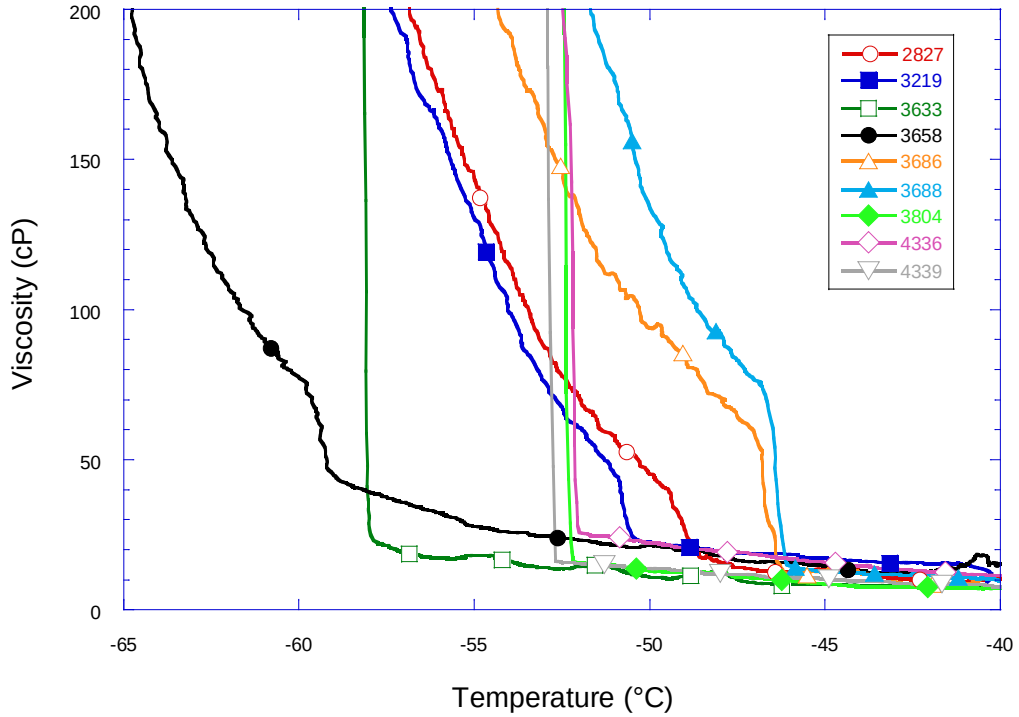

Figure 3. Viscosity behavior of a series of Jet A fuels. The numbered labels shown are AFRL fuel sample numbers.

Viscometer Calibration

As the Scanning Brookfield Viscometer was designed for high viscosity engine oils, new calibration techniques have been developed for jet fuels which have significantly lower viscosities. Early in our prior work with the system, we saw the need for a calibration fluid that was easy to obtain and whose viscosity at relevant temperatures was near the expected range of jet fuels. Traditional oil calibration fluids required high temperatures to reach the lowest viscosity range necessary. We found that 2-propanol, from a sealed dry container, could be used as a calibration fluid at the low temperature and viscosity range of jet fuel. In addition to having a known viscosity and density versus temperature relationship, 2-propanol is inexpensive and readily available. Savant Laboratories has developed a narrow molecular weight mineral spirit hydrocarbon blend which can also be used for viscometer calibration.

It is useful to note that the SBV measures normal or dynamic viscosity, the ratio of shear stress (F/A) to the velocity gradient, ($\Delta v_x/\Delta z$), while the more common kinematic viscosity is determined from flow through a capillary tube. The two measurements are related to each other by the fluid density. When the SBV results are compared to kinematic viscosity measurements, performed using capillary viscometer tubes, it is useful to anchor the SBV results to a single temperature kinematic viscosity measurement. This anchoring technique requires an accurate value of the fuel density at the anchoring temperature. Figure 4 shows an example of density measurements obtained at low temperatures using a pycnometer and low temperature bath. As the figure shows, the change in density over the change in temperature, i.e., the slope of the data, is both linear and consistent for a variety of hydrocarbon fuels regardless of the absolute density. The predictable temperature dependence of density allows low temperature density predictions of fuels with limited data. Thus the conversion of dynamic to kinematic viscosity is a simple linear transform.

For all measurements reported here, the SBV results were anchored to a capillary viscometer measurement at -40°C. In addition, Tannas Co. Newtonian Oil LNF-45 was used for calibration of the torque viscosity behavior of the SBVviscosity head.

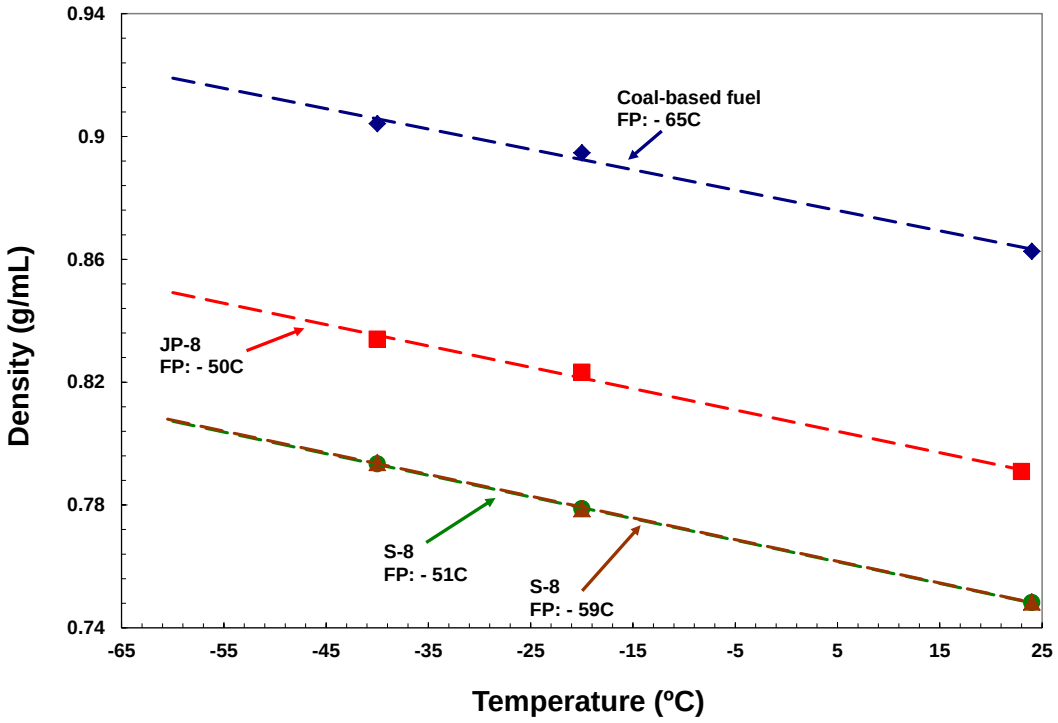

Figure 4. Density vs. temperature plots for four fuels obtained using a pycnometer.

Selection of Rheological Parameters

An important goal of this project is the selection of a rheological parameter that allows prediction of the flowability and pumpability of fuel during aircraft operation. One possible parameter is the temperature at which the "knee" (sudden increase) in the viscosity curve (see Figure 3 above) occurs upon cooling, T_{knee}. This knee occurs very close to the measured fuel

cloud point as shown in Figure 5 and should provide a good measure of a minimum temperature above which fuel flowability remains satisfactory.

Another parameter that may be useful is the concept of a viscosity “equivalent limit” for freezing point (2). This is a viscosity maximum limit at a defined temperature that is the highest expected viscosity for the current populations of specification fuels. Thus, the low temperature viscosity would be measured for a large population of fuels (e.g., Jet A fuels), at a defined temperature (e.g., -37ºC), and the expected maximum viscosity determined. This viscosity would then be used as the viscosity “equivalent limit” for all Jet A fuels at this temperature.

Another potential rheological parameter is the gelation index, which is part of the ASTM D5133 method. The gelation index is obtained from the first derivative of a moving average of the measured torque curve, and indicates the maximum slope of the viscosity curve. The gelation index was not evaluated for this program, as the maximum slope occurs at temperatures below the beginning of fuel crystallization. This is a two-phase region, where solid crystals coexist with liquid-phase fuel. In addition, the relationship between gelation index and flowability is not well defined.

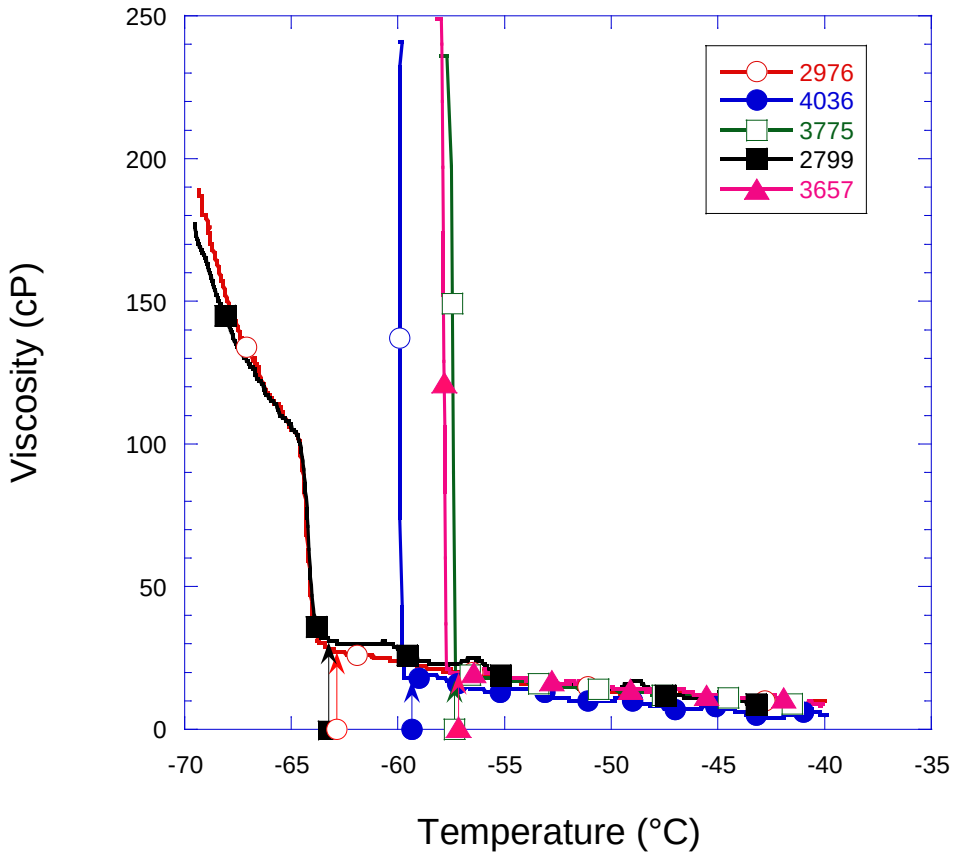

Figure 5. Plots of viscosity vs. temperature for five jet fuels showing that the cloud point occurs near the viscosity knee temperature. The cloud points for each fuel are indicated by arrows pointed to the viscosity curve from the x-axis.

Atypical Viscosity vs. Temperature Behavior Considerations

The vast majority of qualified petroleum-derived jet fuels display well behaved viscosity vs. temperature profiles when using the SBV method. However, there is reason to believe that some fuels will exhibit unusual viscosity profiles. For example, the low temperature (LT) flow improving additive developed for the JP-8+100LT program is known to eliminate the "knee" (rapid rise) in the viscosity vs. temperature profile of fuels to which it is added as shown in Figure 6. Instead of a rapid rise in viscosity as temperature is decreased, these fuels exhibit a gradual increase in viscosity with reduced temperature. Depending on the viscosity parameter selected, such behavior may make determination of this parameter difficult or impossible. Other fuels may also exhibit unusual viscosity vs. temperature behavior, including alternative fuels, fuels containing drag reducing additives, and fuels with diesel or biodiesel contamination.

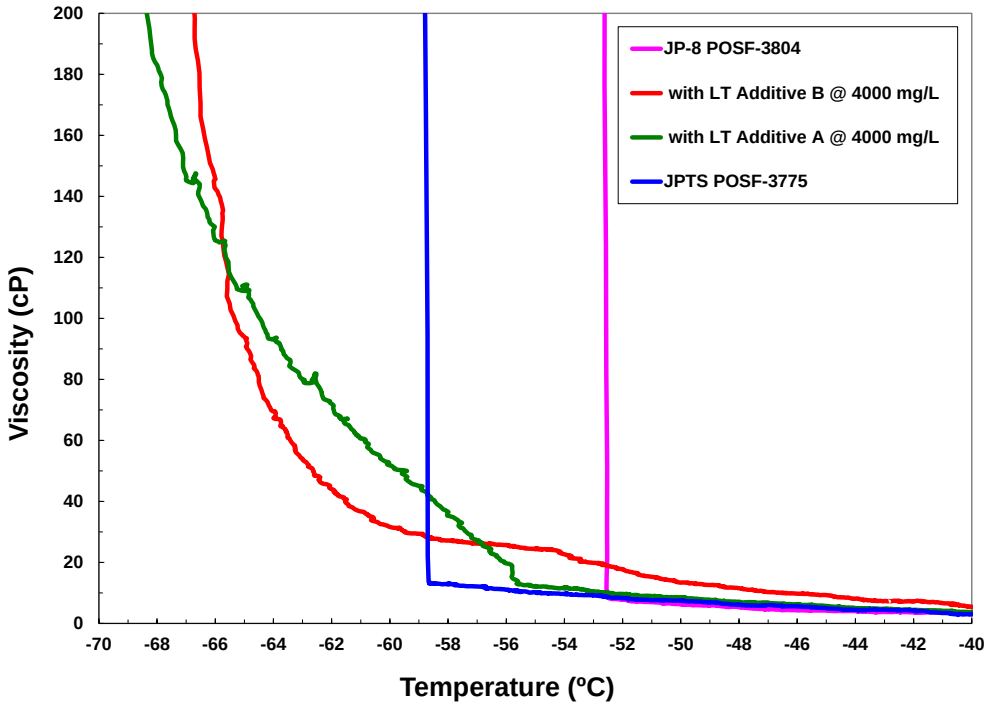

Figure 6. Scanning Brookfield Viscosity data showing the effect of two low temperature flow improving additives on the viscosity vs. temperature profile of a JP-8 fuel (freezing point of -47.6°C). Also shown is a low freezing point JP-TS fuel for comparison (freezing point of -54.1°C).

Cooling vs. Heating Hysteresis

Different viscosity vs. temperature profiles are obtained when the SBV instrument is evaluated during cooling and heating. An example of these differences is shown in Figure 7 for a Jet A fuel with a freezing point of -55.1°C. It is apparent that upon warming the viscosity does not decrease as rapidly with temperature as it rises upon cooling. These different observed behaviors on cooling and heating also need to be considered when selecting a viscosity-based specification method to correlate with the freezing point specification. The figure also shows that during

warming the viscosity curve returns to match the cooling curve very close to the -55.1°C freezing point. This observation makes sense when one considers that the increase in viscosity during cooling is due to formation of crystals along with the fact that the freezing point is defined as the temperature where the last crystal is melted upon heating. Thus, one expects the heating and cooling viscosity curves to coincide above the freezing point temperature, where only a single liquid-phase is present.

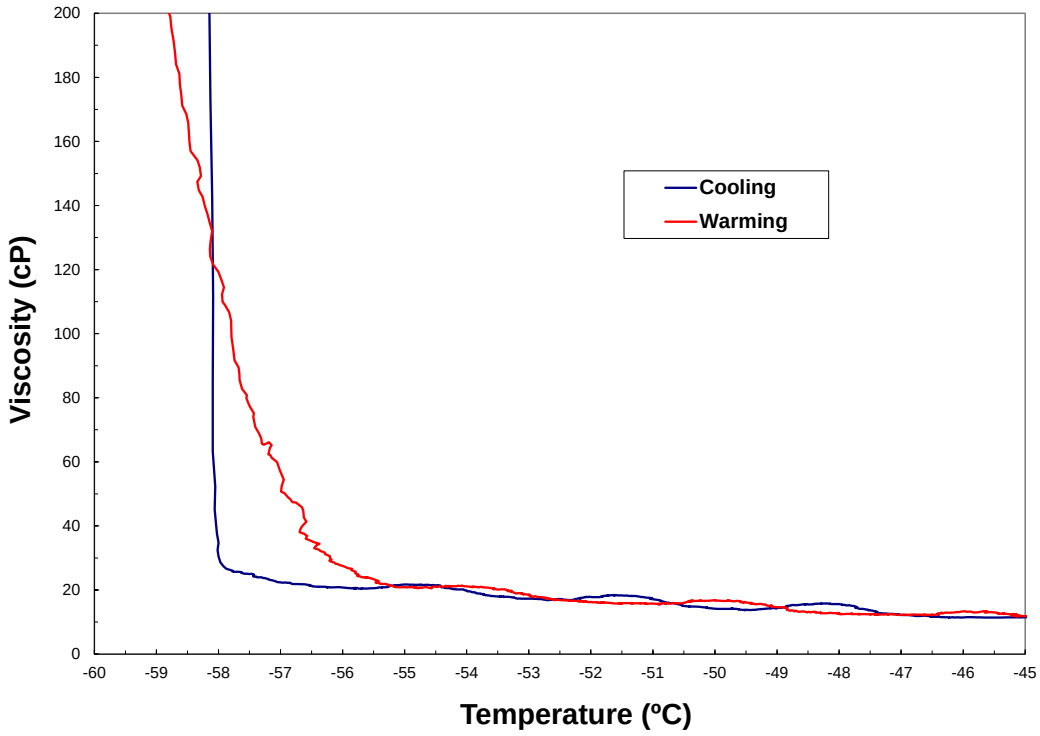

Figure 7. Plots of viscosity vs. temperature for a Jet A fuel (POSF-3633, freezing point= -55.1°C) showing differences in profiles obtained during cooling and heating.

Viscosity vs. Freezing Point as a Low Temperature Fuel Specification

The desire to move towards a low temperature fuel specification that better relates to flowability and pumpability creates some uncertainties about how this change would affect the population of fuels that pass the new specification. In particular, there is the uncertainty of the ability of current on-spec fuels to pass the new specification and the possibility that currently off-spec fuels might pass the new specification method. Any new flowability pass-fail specification would have to take into consideration the desire of the fuels community to either: (1) enforce the current freezing point specification (or some rheology parameter that correlates to freezing point) so that all current fuels pass the new specification and no new fuels pass, or (2) relax (or eliminate) the current freezing point specification and allow fuels based on the agreed flowability properties. Enforcing the current freezing point specification with a viscosity equivalent limit is predicated on developing a meaningful correlation, which will not be universal for all fuels. Eliminating the current freezing point limit will likely allow some fuels to pass the new specification that would not meet the current freezing point limit, and may also prevent some fuels from passing the new

specification that currently do pass the freezing point limit. Industry stakeholders will need to consider these issues prior to implementation of a new low temperature specification.

Project Approach

The main goal of this project was to provide a specification test parameter, based on viscosity measurements, which more closely correlates to fuel flowability and pumpability in aircraft and engine operations at low temperatures. Initially, freezing points and viscosity curves were measured for a wide range of Jet A, Jet A-1, and JP-8 fuels. These measurements were performed specifically for this program, although we have been able to augment these data with historical data that have previously been measured on AFRL sponsored programs.

Two proposed viscosity parameters have been explored in this study. These are the viscosity "knee temperature" and the viscosity "equivalent limit." We have also explored the limitations of these proposed viscosity parameters. Such limitations may involve viscometer calibration issues, heating/cooling viscosity hysteresis, behavior of alternative fuels, effect of additives and contaminants.

Another goal of the program was to measure fuel n-alkane distributions and correlate with freezing point and viscosity parameter to show the maximum possible n-alkane content which passes the new viscosity specification method. This was suggested as an increased large n-alkane content may influence combustor spray atomization and relight (2). We have employed a combination of GC-MS and GC-FID to separately quantify the higher concentration and lower concentration n-alkanes, respectively. The higher concentration n-alkanes are less well separated from interfering species, and the use of the MS detector in single ion mode enables their separation and quantification.

Scanning Brookfield Viscometry Correlation to Freezing Point

Initial work on the program involved generating Scanning Brookfield Viscosity (SBV) and freezing point (FP) results over a range of jet fuel samples. We also obtained measured SBV and FP results on runs conducted for previous AFRL low temperature fuel research programs. The SBV runs include 27 "older" runs conducted from 2002 to 2011, and 26 "newer" runs conducted in 2012 for the current program. These new runs were performed on 26 unique fuel samples covering Jet A (13 samples), Jet A-1 (2 samples), and JP-8 (11 samples) fuels. The FP runs were performed using ASTM D5972, Standard Test Method for Freezing Point of Aviation Fuels (Automatic Phase Transition Method). This method offers the best precision of the four approved methods listed in jet fuel specification ASTM D1655, namely:

- D2386, Test Method for Freezing Point of Aviation Fuels
- D5972, Test Method for Freezing Point of Aviation Fuels (Automatic Phase Transition Method)
- D7153, Test Method for Freezing Point of Aviation Fuels (Automatic Laser Method)
- D7154, Test Method for Freezing Point of Aviation Fuels (Automatic Fiber Optical Method)

It should be noted that use of the alternate methods may give slightly different results for freeze point. When multiple runs were performed the results are reported as an average of the individual measurements. A summary of the data obtained is shown in the Appendix in Table A1.

The SBV runs were conducted at a -5°C per hour cooling rate from a starting temperature of -20°C to a final temperature of -70°C, or to a higher final temperature when an 80 cP viscosity is exceeded. An example of an SBV run is shown in Figure 8. The figure shows that the viscosity gradually increases as the temperature is reduced, until -53.9°C where a sudden rapid increase in viscosity is observed. We refer to this sudden increase in viscosity as the viscosity "knee," and to the temperature at which it occurs as the viscosity "knee temperature." Our previous work (8) has shown that the viscosity knee occurs when wax crystal formation begins as a result of the freezing of large n-alkanes in the fuel. We have chosen to explore the use of the viscosity knee temperature as a viscosity equivalent measurement of freezing point.

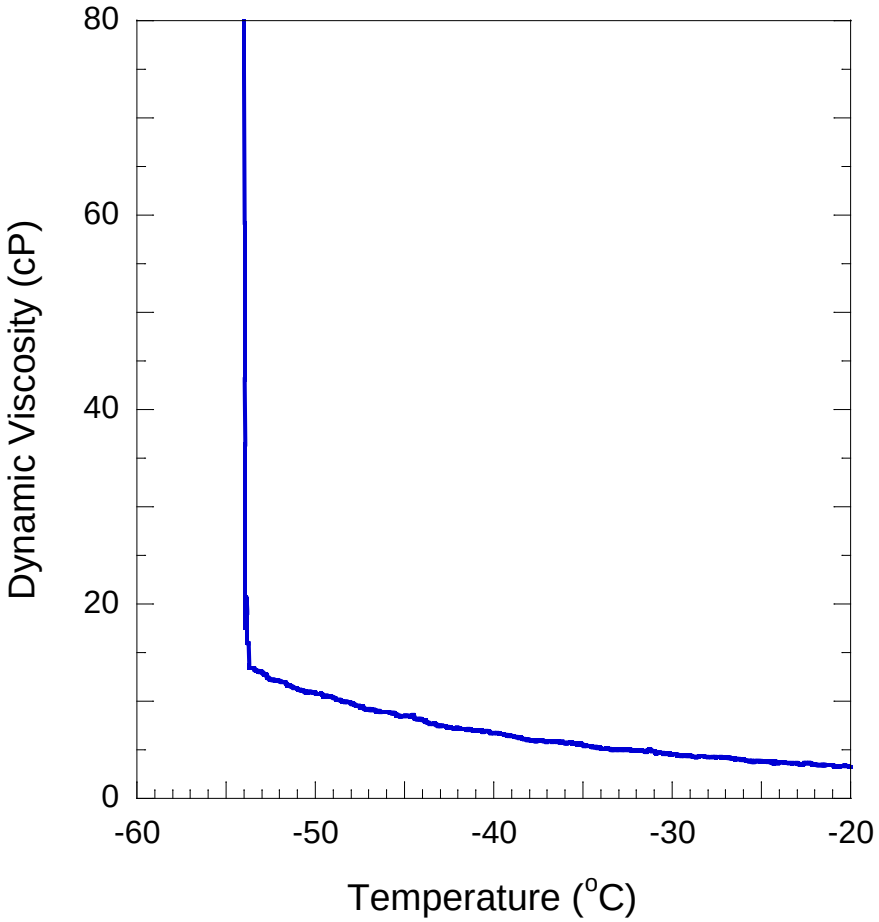

Figure 8. Scanning Brookfield Viscosity results for a JP-8 fuel (POSF-3773) at a cooling rate of -5°C per hour.

To study the usefulness of the viscosity knee temperature, we have plotted this parameter as a function of the measured freezing point for all fuels for which we had both measurements close together in time (within a few months). The results are shown in Figure 9. The figure indicates an excellent linear correlation between FP and the viscosity knee temperature. The linear regression best fit line is:

Knee temperature (°C) = (0.954 * FP) - 5.70,

with an R^2 goodness of fit parameter of 0.977. This correlates to a knee temperature of -43.9°C at the -40°C Jet A freezing point specification, and a knee temperature of -50.5°C at the -47°C Jet A-1/JP-8 FP specification. The data show that the FP can be predicted by the measured viscosity knee temperature to a precision of ±2°C.

As the data exhibit a fitted slope very near unity, the data fit can be forced to a slope of one, yielding the fit,

Knee temperature (°C) = FP - 3.32.

This fit shows a very slightly reduced R^2 goodness of fit of 0.957. The excellent correlation of this fit indicates that, within the experimental uncertainty, there is a simple temperature offset between the viscosity knee and FP temperature of ~3.3°C over a range of fuels and fuel types.

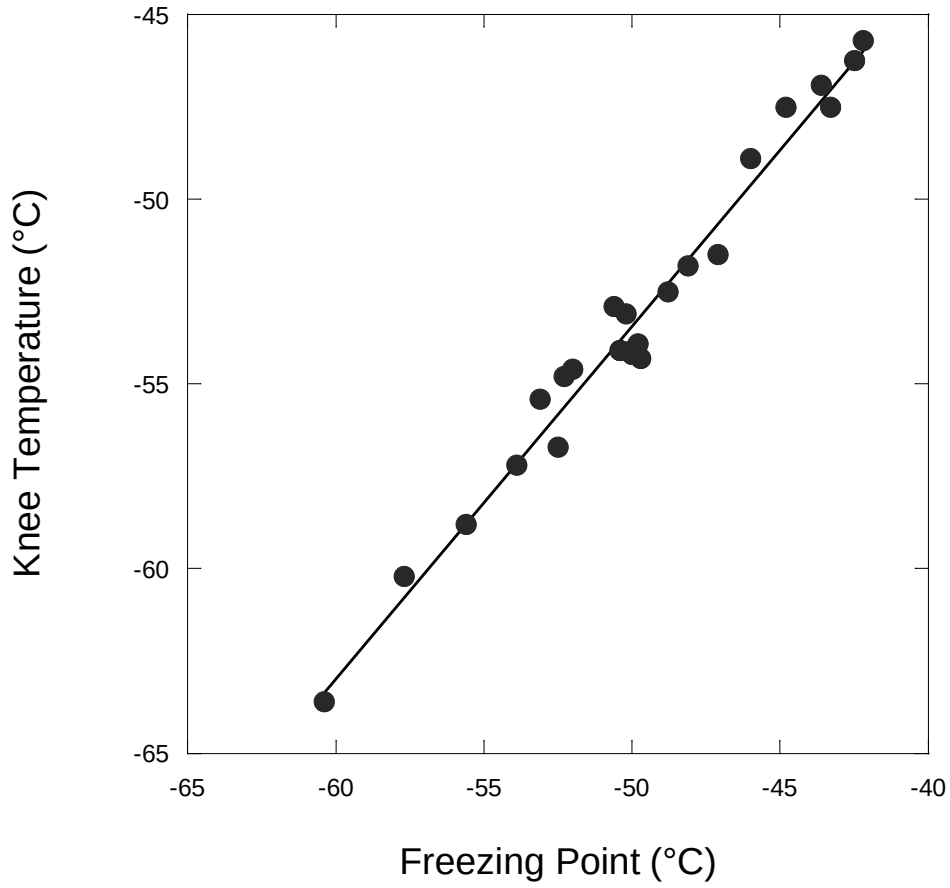

Figure 9. Plot of viscosity knee temperature vs. freezing point for a range of Jet A, Jet A-1, and JP-8 fuels.

Figure 10 shows the same data, but here we have plotted and fit the Jet A fuels (-40°C FP spec) separately from JP-8/Jet A-1 (-47°C FP spec) fuels. The figure shows that the fitted lines are

nearly identical for the two groups of fuels. Also shown in Figure 10 is a vertical line at the -47°C FP specification demonstrating that fuels are typically produced to exhibit freezing points at least 2°C below the specification FP.

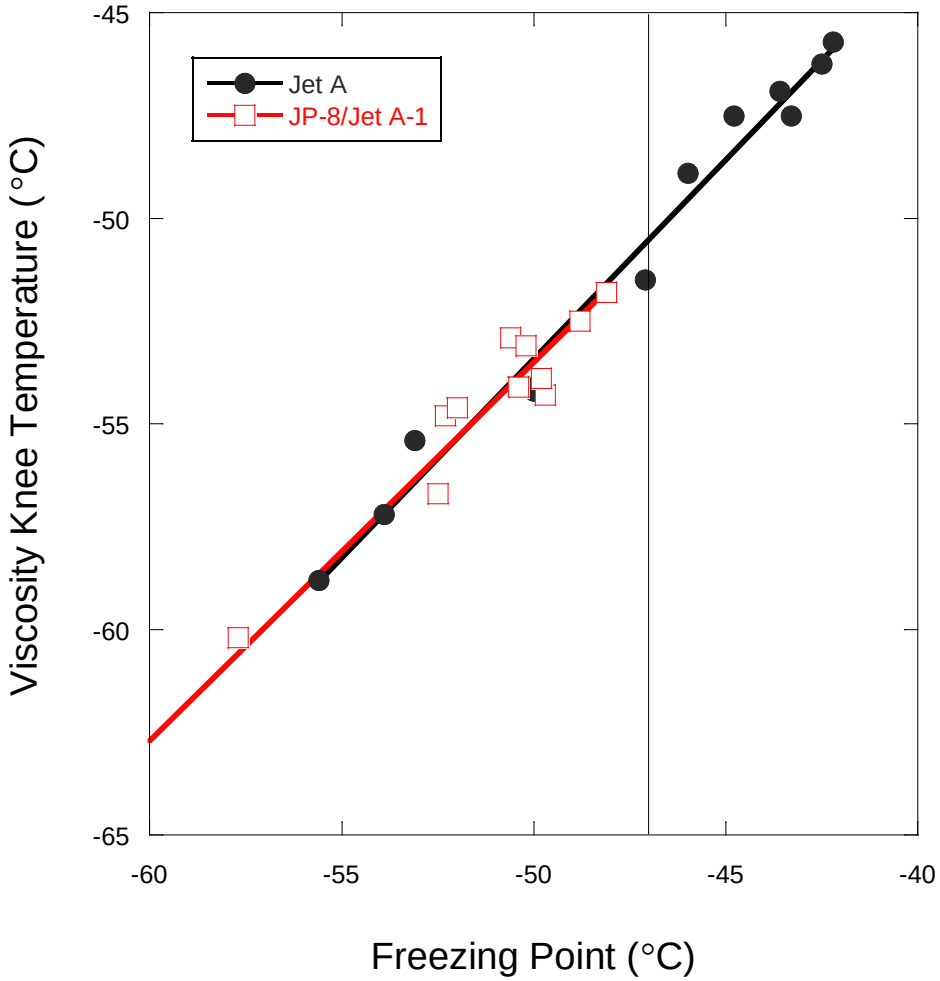

Figure 10. Plot of viscosity knee temperature vs. freezing point for a range of Jet A, Jet A-1, and JP-8 fuels with Jet A fuels grouped separately from JP-8/Jet A-1 fuels.

Repeatability

A successful specification method requires excellent repeatability and reproducibility. It is desirable that a new low temperature fuel specification method exhibits a precision that is at least as good as the current freezing point methods. Table 1 lists the repeatability and reproducibility of current ASTM/IP methods for fuel freezing point. Here we have performed repeatability studies of the scanning Brookfield viscosity knee temperature using two fuels. These repeatability studies demonstrate the level of precision to be expected for repeated measurements on the same fuel performed in the same laboratory. No attempt has been made here to address the between-laboratory precision (i.e., reproducibility) of the technique.

Table 1. Repeatability and Reproducibility of Current ASTM Freezing Point Methods

Method	Repeatability (°C)	Reproducibility (°C)
ASTM D2386/IP 16 Manual method	1.5	2.5
ASTM D4305/IP 422 Simulated freezing point method	1.2	2.6
ASTM D5972/IP 435 Automatic phase transition method	0.5	0.8
ASTM D7154/IP 528 Automatic fiber optic method	0.5	1.9
ASTM D7153/IP 529 Automatic laser method	0.6	0.9

Figure 11 shows five scanning Brookfield runs for JP-8 fuel POSF-4336, a fuel which exhibits a freezing point temperature of -48.0°C. The viscosity data show measurable scatter at the extreme temperatures, with significant scatter occurring in particular at the low temperature, high viscosity region of the curves. The inset of the plot shows an expanded region near the viscosity knee. The knee temperature displays a mean of -51.8 ± 0.2°C, with the stated error being 2σ standard deviation. Interestingly, four of the five runs were performed over a three week period in 2012, while one of the runs (the red curve in the figure) was performed in 2002. The viscosity knee temperature repeatability for this fuel appears to be excellent over a significant period of time.

Figure 12 shows a repeatability study on Jet A fuel POSF-2926 (freezing point= -43.3°C). The plot shows eight replicate runs, with seven of these conducted over a two month period in 2012. The knee temperature for these seven runs is -47.7 ± 0.2°C (2σ standard deviation). The eighth run was performed in early 2011 and yields a slightly higher viscosity knee temperature (-46.4°C). The seven runs show excellent repeatability for measurement of the viscosity knee temperature. The higher measurement for the older sample may be due to the fuel sample changing in time or experimental error, as it is outside the repeatability of the 2012 runs.

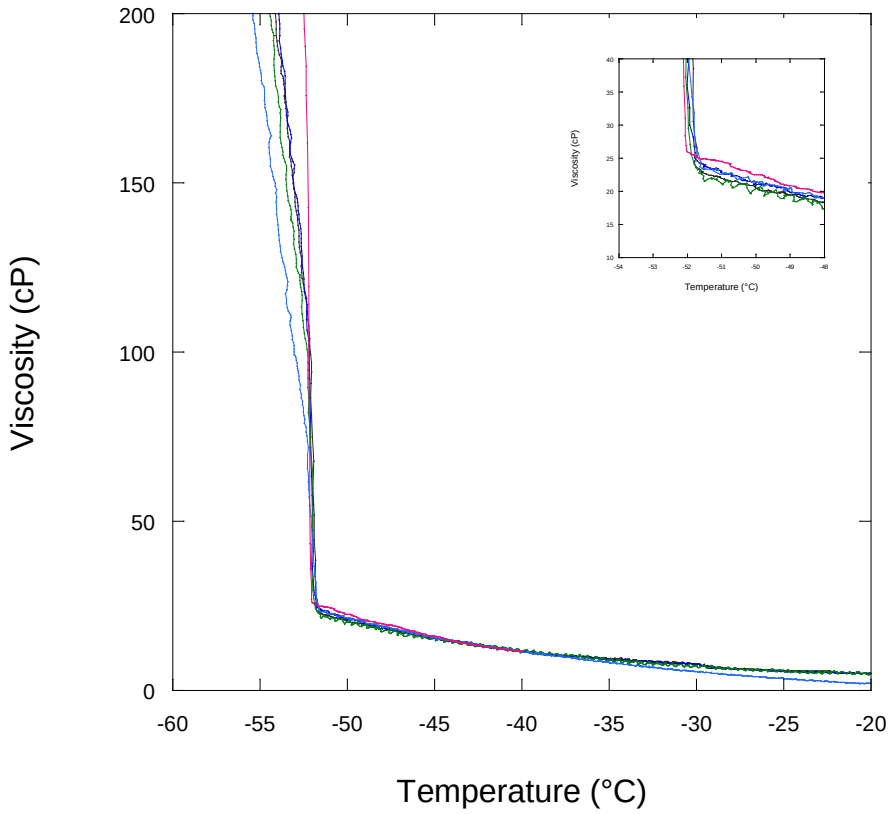

Figure 11. Repeatability study of scanning Brookfield viscosity vs. temperature for JP-8 fuel POSF-4336 (F.P.= -48.0 °C). The plot shows five replicate runs. The inset shows an expanded region near the viscosity knee region.

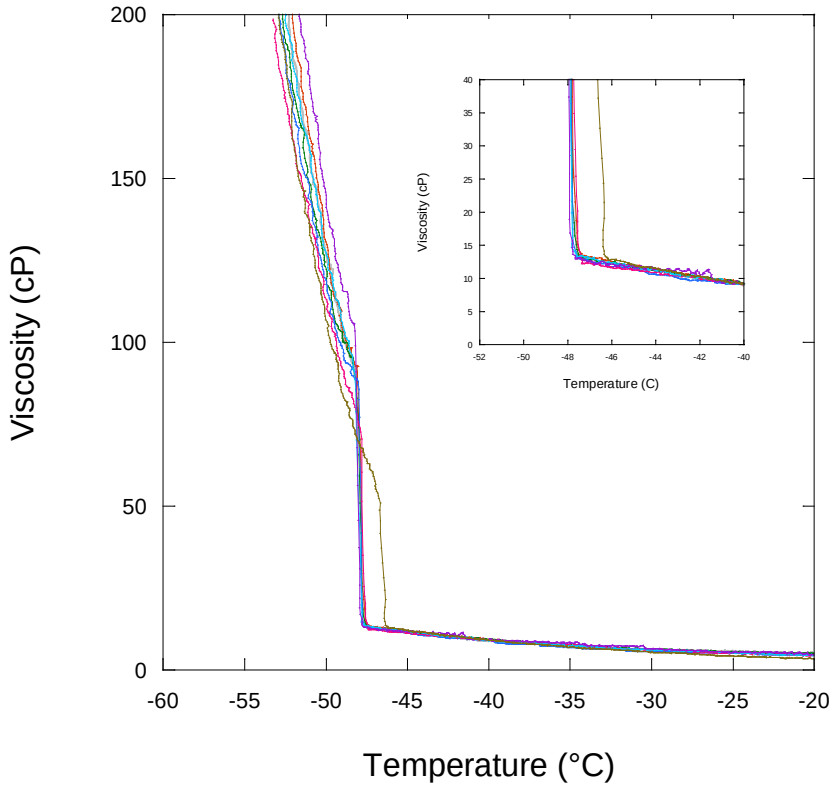

Figure 12. Repeatability study of scanning Brookfield viscosity vs. temperature for Jet A fuel POSF-2926 (freezing point= -43.3°C). The plot shows eight replicate runs. The inset shows an expanded region near the viscosity knee region.

Alternative Fuels

A new low temperature flowability specification method needs to work as well in alternative fuels as it does in conventional (i.e., petroleum-derived) fuels. Here we show scanning Brookfield viscosity results on Fischer-Tropsch derived synthetic paraffinic kerosenes (FT-SPK), hydroprocessed esters and fatty acids derived synthetic paraffinic kerosenes (HEFA-SPK) which are also referred to as hydrotreated renewable jet (HRJ), and alcohol to jet synthetic kerosenes (ATJ). The data are obtained on the neat blend stocks, rather than blends with petroleum-derived jet fuels, to better show the behavior of these alternative blend components.

Figure 13 shows scanning Brookfield viscosity results for four Fischer-Tropsch derived SPK fuels. Table 2 lists the measured freezing points for these fuels and Table 3 lists their n-alkane content. The FT SPK fuels exhibit varying behavior with three of the fuels showing sharp viscosity knee transitions and one fuel (POSF-4909) displaying a smoothly upward curving viscosity with only a barely discernible viscosity knee near -54.5°C with decreasing temperature. One might expect that a low n-alkane content would cause this lack of a viscosity knee, but Table 3 shows that this fuel has 17.2 % n-alkanes. As these FT SPK fuels display n-alkane levels over the range 14.3 to 44.2 weight%, this fuel does not contain an unusual n-alkane content. Interestingly, the fuel with the highest n-alkane level, POSF-5172, displays a relatively low freezing point of -54.2°C despite this high n-alkane content. A closer look at Table 3 shows that nearly all of the n-alkanes in this fuel are n-C_9 to n-C_{11}, with very few of the larger n-alkanes that

increase freezing points. This fuel also exhibits the lowest measured viscosity of the four FT SPK fuels. These results demonstrate the importance of the larger n-alkanes in increasing both viscosity and freezing point.

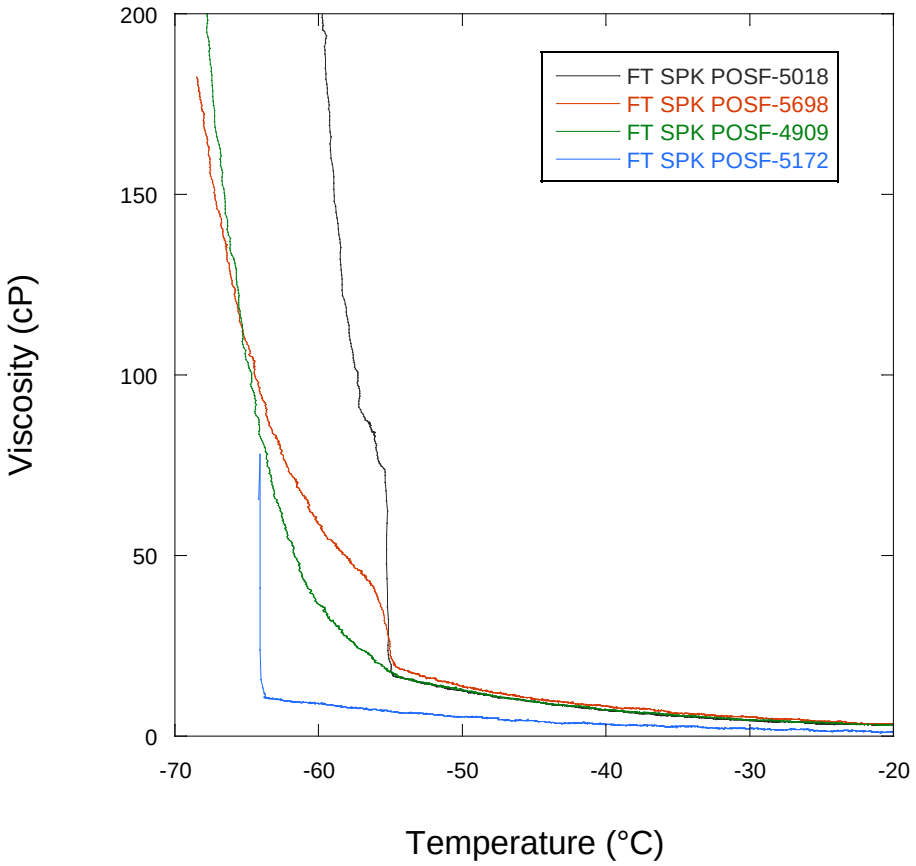

Figure 13. Plots of scanning Brookfield viscosity vs. temperature for four Fischer-Tropsch synthetic paraffinic kerosenes.

Table 2. Measured Freezing Points of Alternative Fuels

Fuel	Producer	Freezing Point (°C)
FT SPK POSF-5018	Syntroleum	-49.4
FT SPK POSF-5698	Rentech	-50.0
FT SPK POSF-4909	Syntroleum	-51.2
FT SPK POSF-5172	Shell	-54.2
HEFA POSF-7449	General Atomics	-58.0
HEFA POSF-6308	UOP	-62.0
HEFA POSF-6866	SAIC/UND/EERC	-63.0
ATJ POSF-6882	Gevo	<-65

Table 3. Measured n-Alkane Content of Alternative Fuels

POSF	Fuel Type	n-Paraffins (wt%)													Total (wt%)
		nC7	nC8	nC9	nC10	nC11	nC12	nC13	nC14	nC15	nC16	nC17	nC18	nC19	
5018	FT-SPK	0.012	1.20	3.55	4.41	4.32	3.63	2.86	1.84	0.97	0.043	0.001	<0.001	<0.001	22.8
5698	FT-SPK	0.007	1.88	2.75	2.22	1.81	1.52	1.40	1.05	0.90	0.64	0.071	0.002	<0.001	14.3
4909	FT-SPK	0.141	1.32	2.60	3.23	3.18	2.46	1.94	1.18	0.70	0.35	0.090	0.010	0.002	17.2
5172	FT-SPK	0.012	1.63	17.2	20.8	4.14	0.36	0.003	0.001	<0.001	<0.001	<0.001	<0.001	<0.001	44.2
7449	HEFA	0.013	0.07	1.01	0.91	0.77	0.66	0.35	0.27	0.68	0.13	0.001	<0.001	<0.001	4.8
6308	HEFA	<0.001	0.12	2.01	1.88	1.52	1.25	0.82	0.86	0.35	0.004	<0.001	<0.001	<0.001	8.8
6866	HEFA	0.196	0.59	1.30	1.95	2.09	1.88	1.26	0.89	0.48	0.12	0.012	0.001	<0.001	10.8
6882	ATJ	<0.001	0.001	<0.01	<0.01	<0.01	<0.01	<0.01	0.03	<0.01	<0.01	<0.01	<0.01	<0.01	<0.2

Figure 14 displays scanning Brookfield viscosity results for three HRJ fuels and one ATJ fuel. Two of the fuels display slight viscosity knee behavior (POSF-6866 and POSF-7449), while the other two fuels show no obvious viscosity knee to indicate crystallization. As the freezing point of the ATJ fuel, POSF-6882, was too low to measure (<-65°C), it is possible that a viscosity knee was not observed due to the low temperature limit of the scanning Brookfield viscometer bath. The freezing point of fuel POSF-6308 was also quite low, -62.0°C, which also may be the cause of a lack of a viscosity knee. Table 3 shows that these four fuels exhibit very low n-alkane contents, covering the range <0.2 to 10.8 weight%.

These results show that very low freezing alternative fuels may not exhibit an obvious viscosity knee. The lack of a viscosity knee appears to occur in relatively low freezing point fuels, so the inability to detect the knee may not be a problem for its use as a specification method.

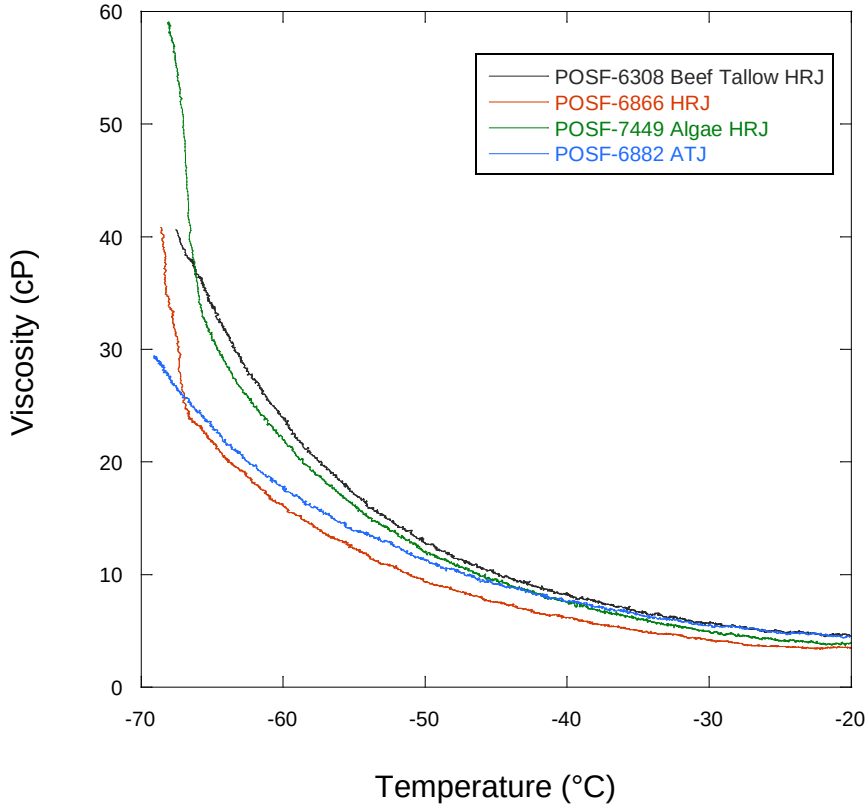

Figure 14. Plots of scanning Brookfield viscosity vs. temperature for four HRJ fuels

Comparison of Scanning Brookfield and Capillary Viscosities near the Fuel Freezing Point

One advantage of using the "knee temperature" as a jet fuel flowability specification is that the scanning Brookfield viscometer does not need to be precisely calibrated for viscosity, as only the temperature measurement is crucial to the result. Temperature is significantly easier to calibrate accurately than is viscosity. Despite this observation, we have chosen to further study the absolute viscosity measurements of the scanning Brookfield viscometer compared with the capillary viscometer at temperatures near the fuel freezing point. As the capillary viscometer has been used for many years to specify jet fuels, it is important to confirm that the SBV method used here yields viscosity measurements that are comparable.

Figure 15 shows a comparison of scanning Brookfield viscometer measurements with capillary viscosity measurements via ASTM D445. The measurements were performed for 12 fuels (Jet A, JP-8, F-T, ATJ Blends, F-T Blends, and Jet A-1) at a temperature no more than 3ºC above the freezing point of each fuel. The dynamic viscosity measurements were anchored at the -40 ºC viscosity of each fuel as described previously. The dynamic viscosity measurements were converted to kinematic viscosity by dividing by the density of each fuel at the relevant temperature. The densities were obtained from interpolation of density vs. temperature data obtained over a range of temperatures via a pycnometer. The measurements were performed no more than 3ºC above each fuel's freeze point to be near the "knee temperature," but also to ensure that we are in a single liquid-phase regime. The figure also includes a y=x line to indicate a perfect correspondence between the two methods. The measurements show that these fuels cover a range of viscosities (7 to 23 cSt) near their freezing points. The comparison shown in Figure 15 indicates that there is an excellent correlation between the two methods. There does appear to be a slight tendency for the SBV measurements to be on the high side, but this is always less than 1 cSt for all fuels, with an average difference of 0.4 cSt.

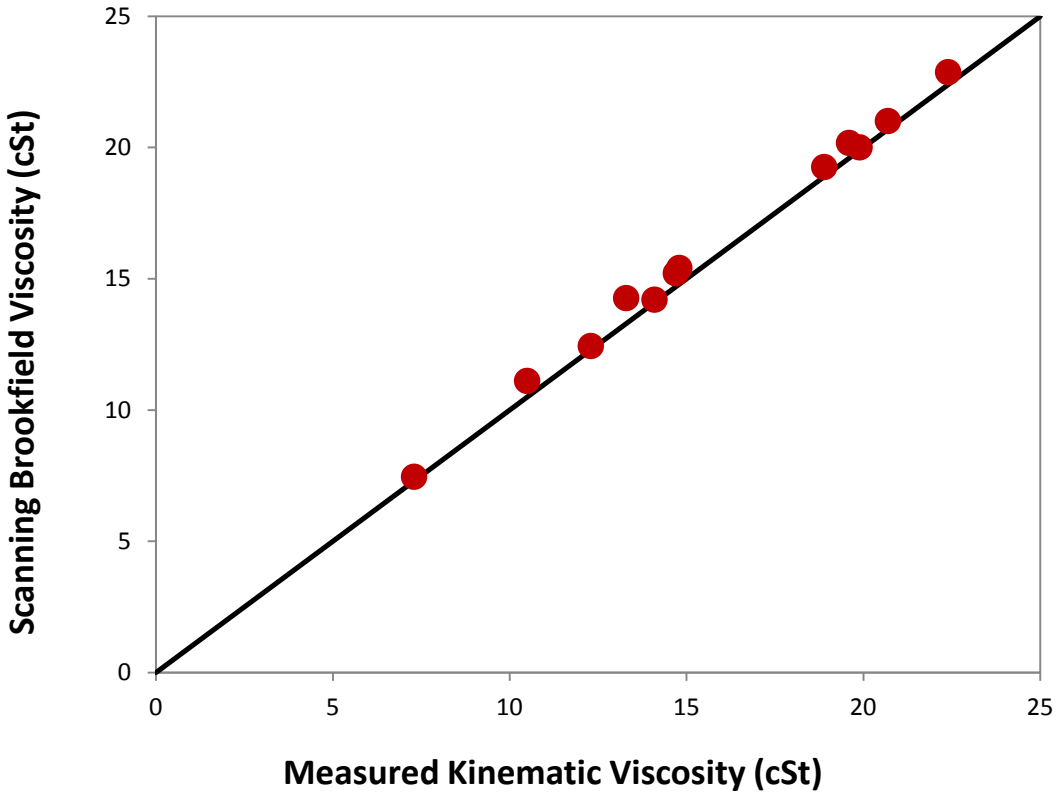

Figure 15. Plot of measured scanning Brookfield viscosity converted to kinematic viscosity vs. measured kinematic viscosity (via capillary viscosity) for 12 fuels at temperatures near each fuel's freezing point.

Jet A Fuel POSF-3658

One petroleum Jet A fuel, (POSF-3658, T_{fp} = -55.7°C) exhibited atypical viscosity behavior compared to the other 25 petroleum fuels evaluated. Figure 16 shows the SBV profile for this fuel and no viscosity knee is obvious, although there is a slight change in slope near -58°C. What is so different about this fuel that causes it not to exhibit a viscosity knee upon cooling? The histogram shown in Figure 17 demonstrates that the 26 petroleum fuels evaluated show a range of n-alkane content from ~6 to 31 wt%. Fuel POSF-3658 exhibits the lowest total n-alkane content (6.1 wt%) of all the petroleum fuels evaluated and contains a below average amount of higher molecular weight n-alkanes (see Table A2). As was the case for the alternative fuels, the reduced amount of n-alkanes, and high molecular weight n-alkanes in particular, results in minimal amounts of wax crystallization. Thus a smooth increase in the viscosity is observed rather than the obvious viscosity knee observed for most petroleum fuels.

An additional peculiarity of fuel POSF-3658 is that it exhibits the highest viscosity of all 26 fuels, even with the lowest total n-alkane content. Again, examination of the n-alkane distribution (Table A2) shows us that this fuel contains the lowest quantity of low molecular weight n-alkanes of the measured fuels. These results suggest that the low molecular weight n-

alkane species are important contributors toward lowering the overall fuel viscosity, which is in contrast to the high molecular weight n-alkanes contributing to an increased viscosity.

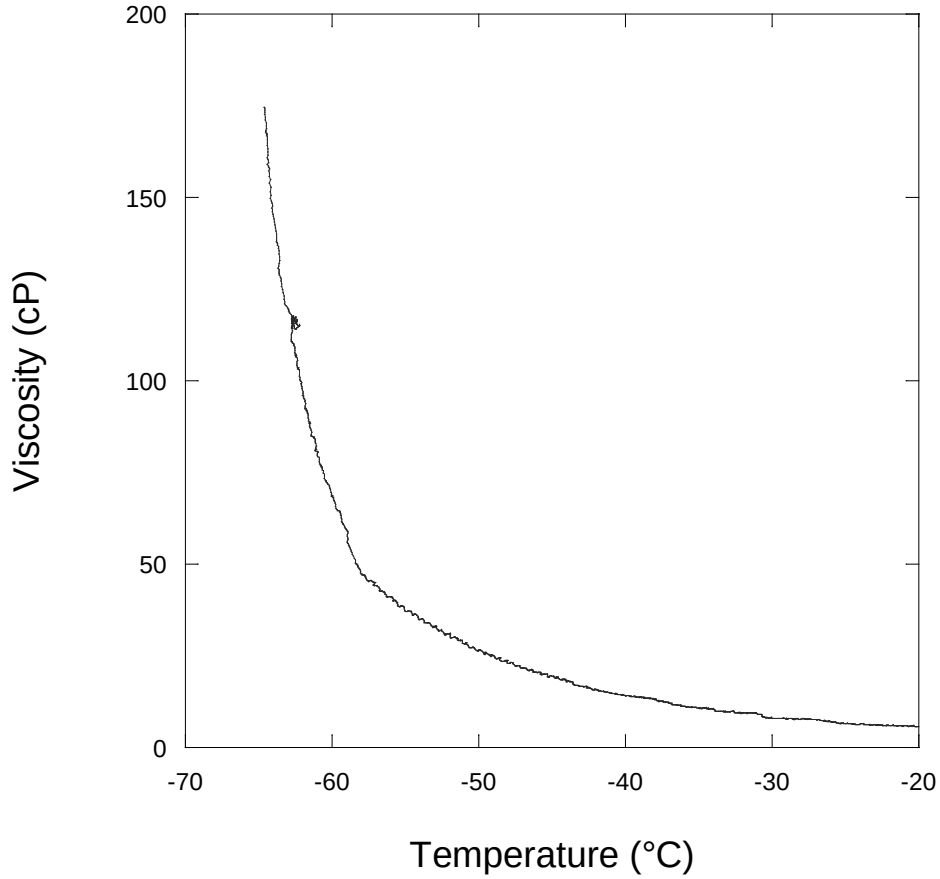

Figure 16. Plots of viscosity vs. temperature for Jet A fuel POSF-3658.

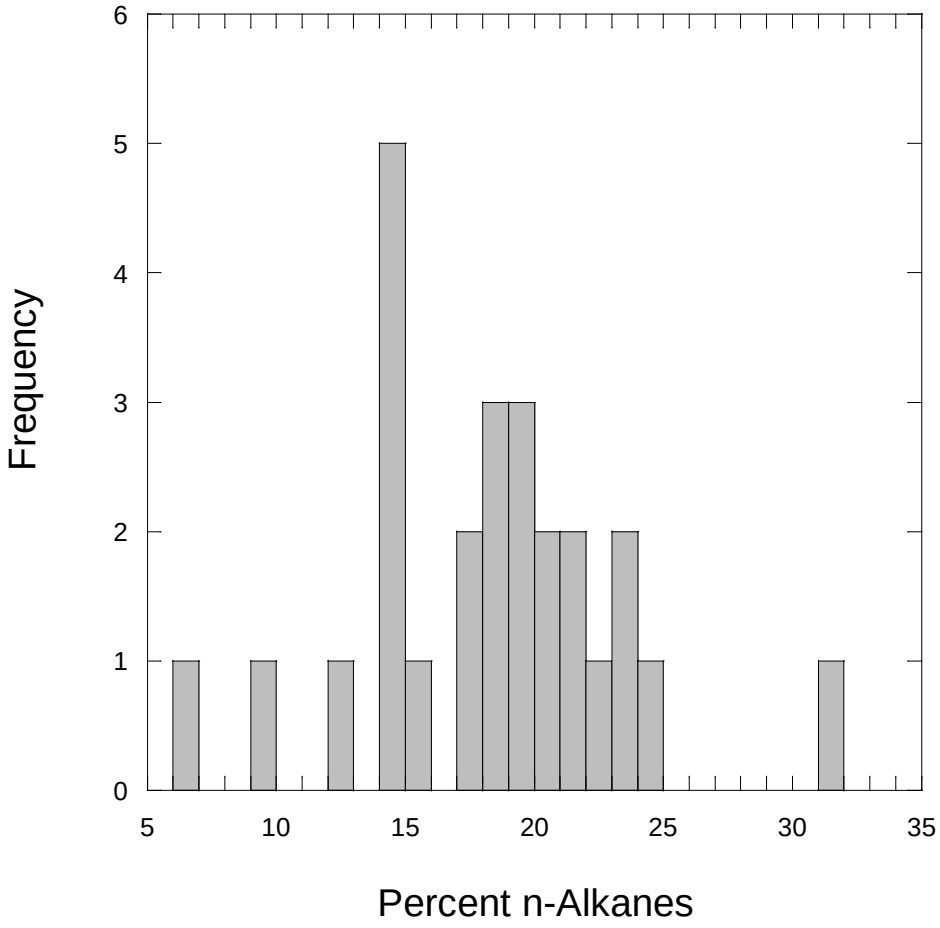

Figure 17. Histogram plot of percent n-alkanes for 26 fuels.

Development of a Viscosity "Equivalent Limit"

It has been suggested that the current freezing point specification limit could be replaced by a viscosity "equivalent limit" (2). This "equivalent limit" would be determined by the viscosity properties of currently acceptable fuels, i.e., fuels that pass the current jet fuel specifications. Thus, one would need to determine the range of viscosities of a large population of currently acceptable fuels at a defined temperature or range of temperatures. These data would indicate the acceptable range of viscosities at a defined temperature – a maximum viscosity limit could then be selected that is slightly greater than the maximum of this range of measured viscosities.

Here we attempt to utilize the above methodology along with the SBV measurements to determine possible viscosity "equivalent limits" for Jet A and JP-8/Jet A-1 fuels. The viscosity data used for this analysis are shown in Table 4. The table shows measured kinematic viscosities for 26 fuels (Jet A, JP-8, and Jet A-1) determined at four temperatures: -20, -37, -40, and -44°C. The -20°C viscosities were measured via capillary viscometry (ASTM D445), while the -37, -40, and -44°C viscosities were measured via SBV (ASTM D5133). The SBV scans were used to extract viscosities at the individual temperatures of interest. The dynamic viscosities were converted to kinematic viscosities by dividing by the measured densities of each fuel. The

densities were determined via extrapolation or interpolation of densities measured at two or three temperatures (typically 15, -20, and -40°C) for each fuel.

The -20°C viscosity column shows that fuel viscosities cover a range of 3.9 to 6.7 cSt with an average of 4.8±0.7 cSt. Each of these fuels passes the 8.0 cSt at -20°C maximum limit, as well as their respective freezing point specification limits.

The fuel viscosities were evaluated at their minimum allowed operating temperatures (2, 27), i.e., 3°C above their specification limit freezing point. Thus the Jet A fuels were evaluated at -37°C (-40°C freezing point + 3°C) and the Jet A-1/JP-8 fuels were evaluated at -44°C (-47°C freezing point maximum + 3°C). All of the fuels were also evaluated at -40°C which is the Honeywell APU low temperature starting and operation limit for commercial Jet A-1 use. All viscosities that are over 12.0 cSt are shown in red in the table. These data were highlighted as Honeywell considers 12 cSt to be the limit for start and operation of their APU's and small propulsion engines, and GE Aviation considers 12 cSt to be their most severe starting limit at -40ºC and lower (2).

The ranges and averages of these measured viscosities are summarized in Table 5. The table shows that the -37°C viscosities for Jet A fuels cover the range 6.4 to 14.4 cSt with an average of 9.2±2.0 cSt. The Jet A-1/JP-8 -44°C viscosities cover the range 9.6 to 17.3 cSt with an average of 11.8±2.5 cSt. The -40°C viscosities of all 26 fuels cover the range 7.4 to 16.9 cSt with an average of 10.2±2.2 cSt. It is apparent from Table 4 that a significant fraction of the fuels exceed the 12.0 cSt at each of these temperatures. It is also apparent that viscosity "equivalent limits" would have to be at least 14.4, 16.9, and 17.3 cSt at -37, -40, and -44°C, respectively. It is important to keep in mind that the limits obtained here are for a relatively small number of fuels and that measurement of a much larger population of fuels would be required to determine a final viscosity "equivalent limit."

Table 4. Measurements of Freezing Point, Viscosity Knee Temperature, and Kinematic Viscosity at Various Temperatures

POSF	Fuel Type	T_{fp} (°C)	T_{knee} (°C)	Kinematic Viscosity (cSt)			
				Capillary	SBV		
				-20°C	-37°C	-40°C	-44°C
2827	Jet A	-50.0	-54.1	4.1	6.4	7.4	
2926	Jet A	-43.3	-47.5	5.4	9.6	10.8	
3084	Jet A	-46.0	-48.9	5.0	8.4	10.7	
3166	Jet A	-44.8	-47.5	5.3	9.9	11.3	
3219	Jet A	-47.1	-51.5	5.2	9.3	10.7	
3602	Jet A	-53.9	-57.2	5.0	8.9	10.6	
3633	Jet A	-55.6	-58.8	4.0	7.4	7.7	
3638	Jet A	-53.1	-55.4	3.9	6.9	7.7	
3658	Jet A	-55.7		6.7	14.4	16.9	
3683	Jet A	-42.2	-45.7	5.4	10.3	11.9	
3686	Jet A	-43.6	-46.9	5.6	10.3	12.2	
3688	Jet A	-42.5	-46.25	4.8	9.5	10.7	
3694	Jet A	-50.0	-54.2	4.5	8.1	9.6	
2747	Jet A-1	-60.4	-63.6	4.1		8.2	9.8
4877	Jet A-1	-52.3	-54.8	4.2		8.5	10.1
3773	JP-8	-49.7	-54.3	4.1		8.1	9.5
3804	JP-8	-48.8	-52.5	4.2		8.3	10.0
4177	JP-8	-57.7	-60.2	4.9		10.2	12.3
4336	JP-8	-48.1	-51.8	5.9		13.7	17.3
4339	JP-8	-50.6	-52.9	4.3		8.7	10.7
4351	JP-8	-52.5	-56.7	5.9		13.0	15.8
4751	JP-8	-50.2	-53.1	4.9		9.9	12.0
4908	JP-8	-50.4	-54.1	5.1		11.0	13.6
4911	JP-8	-52.0	-54.6	4.8		9.4	11.9
5699	JP-8	-50.4	-54.1	4.0		7.9	9.9
6169	JP-8	-49.8	-53.9	4.2		8.5	10.2

Table 5. Measured Kinematic Viscosities at Minimum Operating Temperatures for 26 Fuels

Fuel & Temperature	Minimum Kinematic Viscosity (cSt)	Maximum Kinematic Viscosity (cSt)	Average Viscosity & 1σ Standard Deviation (cSt)	Maximum Prediction Interval (95%) Viscosity (cSt)	Maximum Prediction Interval (99%) Viscosity (cSt)
Jet A Fuels (-37°C)	6.4	14.4	9.2±2.0	13.6	15.5
All Fuels (-40°C)	7.4	16.9	10.2±2.2	15.6	17.7
JP-8/Jet A-1 Fuels (-44°C)	9.6	17.3	11.8±2.5	18.7	21.4

The analysis above uses the maximum observed viscosity for a finite number (≤26) of jet fuel samples to determine maximum viscosity limits at specific temperatures. An alternative method is to determine statistical Prediction Intervals (PI) for the entire population of 26 fuels over a range of temperatures. Figure 18 shows kinematic viscosity data from the SBV on a logarithmic scale at every degree for all 26 fuels as a function of inverse temperature. It can be seen that both the Jet A and JP-8/Jet A-1 fuels exhibit similar viscosity behavior with overlapping linear trends in the data. Liquid viscosity as a function of temperature is often fitted to the Andrade equation (28-29):

$$\ln(\upsilon) = A + \frac{B}{T}$$

Regression analysis was performed on the data shown in Figure 18 using the form of the Andrade equation shown above. The results of this analysis and the derived 95 Prediction Intervals are shown in Figure 19. The calculated maximum Prediction Interval at a defined temperature can be used to provide an expected viscosity maximum at this temperature. The maximum expected viscosities derived from maximum 95 and 99% Prediction Intervals are shown in Table 5. The 95% Prediction Interval values are slightly different from those based upon the individual measurements, but are always within 1.5 cSt. The 95% Prediction Interval maxima yield viscosity "equivalent limits" that would have to be at least 13.6, 15.6, and 18.7 cSt at -37, -40, and -44°C, respectively. The 99% Prediction Interval maxima yield values of 15.5, 17.7, and 21.4 cSt at -37, -40, and -44°C, respectively.

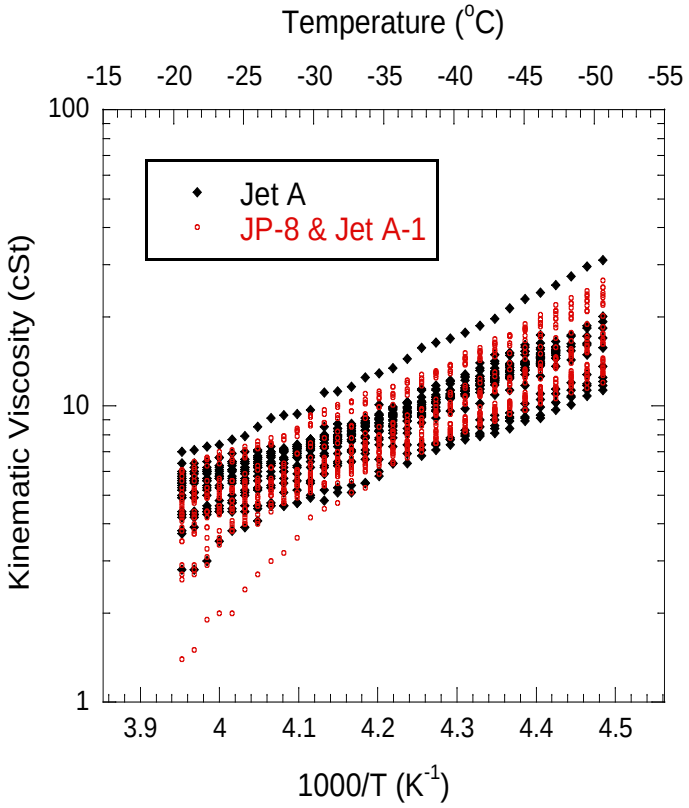

Figure 18. Plots of kinematic viscosity vs. temperature for a range of Jet A and JP-8/Jet A-1 fuels.

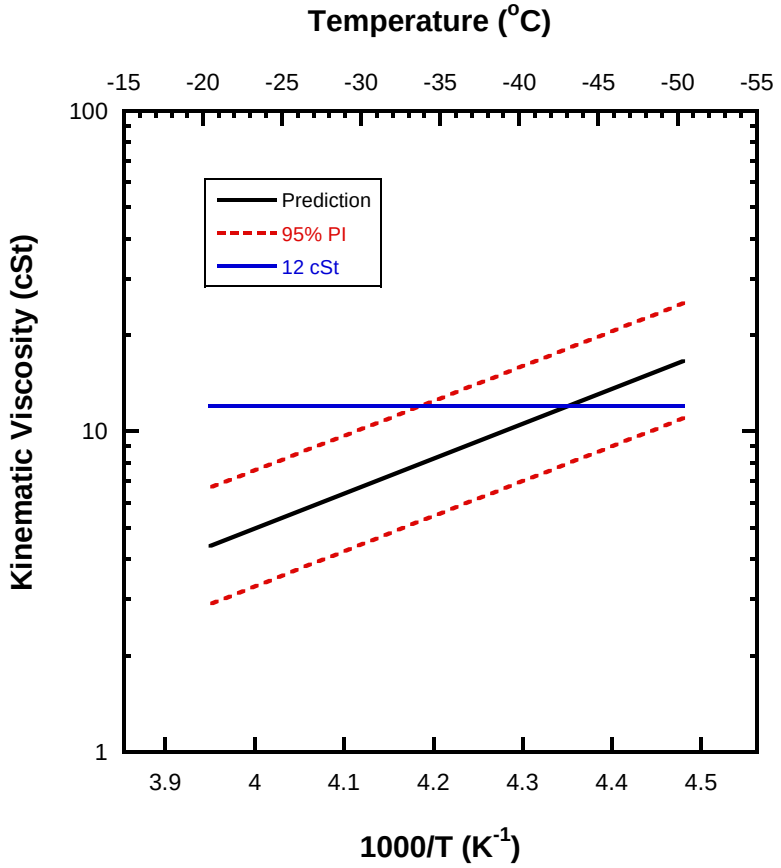

Figure 19. Plots of prediction intervals for the kinematic viscosity of 26 jet fuels.

The low temperature viscosities measured here imply that many fuels exhibit low temperature viscosities significantly above the 12 cSt at -40°C operating limit provided by Honeywell and GE Aviation (2). This may not be an issue for propulsion engines which usually contain inlet fuel/oil heat exchangers upstream of the inlet fuel filter and fuel control. But for APU's and small propulsion engines, which may not have such exchangers, these high viscosities can inhibit proper fuel spray atomization, particularly for high-altitude relight after a long cold soak period. Obviously, input is needed from the engine OEM's for selection of this viscosity equivalent limit for each fuel specification. The relatively high viscosities reported here need to be considered by the OEM's as the data appear to indicate that fuel viscosities during aircraft engine operation may be higher than previously considered.

Correlation of Viscosity to Freezing Point

For all of the petroleum-derived fuels studied here we have attempted to correlate measured freezing point with viscosity. The viscosities were derived at four different temperatures for each fuel: (1) -20ºC, (2) -40ºC, (3) the freezing point temperature of the fuel, and (4) the viscosity knee temperature for each fuel. The results are shown in Figure 20. The results show that the average viscosity increases through the series (-20 ºC, -40ºC, FP, and knee temperature) but there is no apparent correlation between viscosity at any of these temperatures and freezing point.

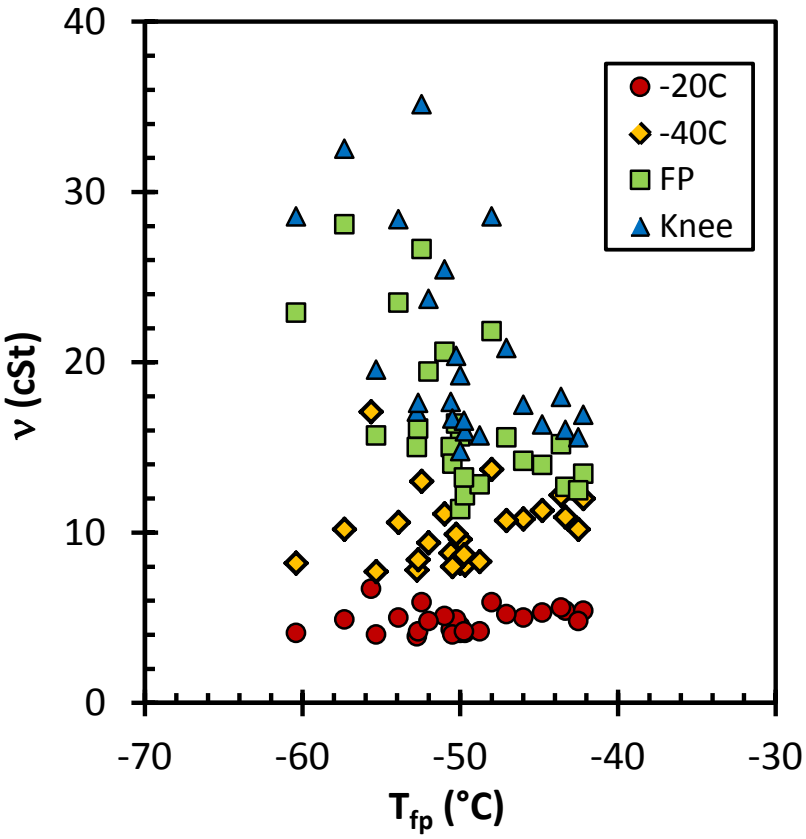

Figure 20. Plots of viscosity at various locations on the SBV curves (-20 and -40ºC, at the fuel freezing point, and at the viscosity knee temperature) vs. freezing point for 26 fuels.

Viscosity of JP-5 Fuels

The current study has concentrated on measurements of Jet A, Jet A-1, and JP-8 fuels. The relatively high viscosities measured at low temperatures cause one to wonder if JP-5, a fuel with a reduced flashpoint for shipboard safety, exhibits even greater viscosity at low temperatures. Due to a higher specification flashpoint (60 ºC vs. 38 ºC for Jet A, Jet A-1, and JP-8 fuels), the JP-5 specification viscosity limit is a maximum of 8.5 cSt at -20ºC, rather than 8.0 cSt for Jet A, Jet A-1, and JP-8 fuels. Table 6 shows the measured kinematic viscosities for eight JP-5 fuels evaluated by the SBV method. The measured viscosities are reported at -40ºC and the -43 ºC operating limit (the freezing point specification limit of JP-5 is -46ºC, and thus the operating limit is three degrees higher). Also included in the table are the measured freezing points and viscosity knee temperatures for these fuels.

The table shows that all of the JP-5 fuels meet the 8.5 cSt -20ºC limit and even the more restrictive 8.0 cSt limit. At -40ºC, half the fuels are above the 12 cSt level, while at the JP-5 operating limit of -43ºC all of the fuels are above 12 cSt. Thus the data indicate that the JP-5 fuels exhibit low temperature viscosities that are greater than measured for the Jet A, Jet A-1, and JP-8 fuels.

Table 6. Measurements of Freezing Point, Viscosity Knee Temperature, and Kinematic Viscosity at Various Temperatures for JP-5 Fuels

POSF	Fuel Type	T_{fp} (°C)	T_{knee} (°C)	Kinematic Viscosity (cSt)		
				Capillary	SBV	
				-20ºC	-40ºC	-43ºC
3939	JP-5	-47.8	-51.5	5.8	12.9	15.6
3940	JP-5	-48.9	-52.6	6.2	14.1	16.6
7983	JP-5	-49.3	-53.0	5.2	11.4	13.5
3461	JP-5	-49.7	-53.1	6.1	14.0	16.6
7932	JP-5	-49.7	-52.8	5.3	11.4	13.3
5095	JP-5	-49.8	-52.8	5.6	12.7	14.8
8632	JP-5	-49.8	-53.0	5.4	11.9	13.9
8133	JP-5	-50.5	-53.6	5.1	10.9	12.8

Discussion on the Viscosity Methods Studied

Viscosity Knee Temperature

Here we have shown the viscosity knee temperature measurement correlates very well with measured freezing point and exhibits excellent repeatability. Some fuels were found to not exhibit viscosity knee behavior, but these were always relatively low freezing point fuels. In addition, some alternative fuels which contained relatively low contents of larger n-alkanes were also found to not exhibit viscosity knee behavior. Thus, the viscosity knee temperature could be used to directly replace the freezing point specification in jet fuel specifications without significantly altering the population of fuels that pass/fail. A major change in the population of approved fuels would not be considered desirable by either fuel users or producers.

But, the main goal of this project was “to provide a specification test parameter, based on viscosity measurements, which more closely correlates to fuel flowability and pumpability in aircraft and engine operations at low temperatures.” As the viscosity knee temperature correlates so closely with freezing point, it is unlikely that this new parameter will provide any additional benefit in correlating more closely to “fuel flowability and pumpability.” In addition, the SBV scans performed here take up to 10 hours to perform, which is significantly longer than any of the specification freezing point methods. Nevertheless, it is expected that somewhat faster scanning (by a factor of two) could provide equivalent results.

Viscosity Equivalent Limit

The viscosity limit measurements and analysis provided here yield viscosity data and maximum limits that can be used to construct a viscosity “equivalent limit” for current specification fuels. These measured low temperature viscosities should directly correlate to operational flowability and pumpability in aircraft engines. But, the calculated maximum limits at various low temperatures imply that fuel viscosities are significantly higher than expected when compared to OEM operability limits. These higher viscosities and their effect on fuel spray atomization will need to be considered by the engine OEM’s. Fortunately, the fuel pumps and the use of fuel/oil

heat exchangers upstream of the inlet fuel filter and fuel control provide heat which will significantly lower fuel viscosities prior to combustor injection via the fuel nozzle. However, APU's and small propulsion engines may not use this heat exchanger. Engine relight after a long cold soak at high altitude, such as for an APU that is turned off during flight, may provide a "worst case" for a fuel viscosity specification "equivalent limit."

Relaxing the Specification

Previous reports have surmised that moving from a freezing point specification to a viscosity specification might allow higher freezing points fuels to pass the specification than are currently permitted (2). This is because fuels with asymmetric n-alkane distributions (i.e., with a relatively high level of large n-alkanes, e.g., n-C_{16} to n-C_{19}) will typically exhibit a high freezing point relative to their low temperature flowability characteristics. These fuels may have relatively low viscosities, as viscosity is due to the bulk fuel composition and is less sensitive to low concentration species, such as the large n-alkanes. Thus, including both viscosity and freezing point methods in jet fuel specifications is desirable.

It has also been postulated that use of a viscosity specification near the fuel freezing point temperature would allow OEM's to be less conservative with low temperature use limits and thus allow a relaxing of the viscosity specification (2). This might result in fuels that currently fail the freezing point specification, being allowed via the viscosity specification. But, the data reported here indicate that the current freezing point specification provides fuels with low temperature viscosities that are significantly higher than the OEM operating limits. Thus, it is unlikely that moving to a viscosity specification would result in a relaxing of low temperature fuel specifications.

Contamination Detection

Some of the freezing point measurement methods have been shown to be able to detect contamination from small amounts of higher molecular weight petroleum products, such as diesel fuels and heating oils (30). Viscosity is a parameter that tends to be more sensitive to the fuel constituents that are in higher concentration, rather than low concentration contaminants (29). Thus a viscosity specification is less likely to successfully detect the presence of such contaminants. This is another reason why it is desirable to retain both viscosity and freezing point specifications for jet fuels. One alternative is to eliminate the freezing point specification, but replace it with the SBV knee temperature. The results here show excellent correlation between these two methods. Thus, the scanning Brookfield viscometer could be used to replace both the capillary viscometer and the freezing point apparatus. Use of the knee temperature to replace freezing point would require testing of a larger number of fuels than is reported here to generate an improved correlation. Also, the knee temperature method would need to be evaluated for its ability to detect fuels with relatively high levels of n-alkanes and/or with diesel and heating oil contamination.

References

1. IATA Technical Fuel Group Task Force, "Fuel Freezing Point Harmonisation," IATA Final Report, 2008.

2. Coordinating Research Council, "Develop and Aviation Fuel Cold Flowability Test to Replace Freezing Point Measurement," CRC Report AV-11-09, 2010.

3. J. S. Ervin, S. Zabarnick, K. E. Binns, G. Dieterle, and C. Obringer, "Investigation of the Use of JP-8+100 with Cold Flow Enhancer Additives as a Low-Cost Replacement for JPTS," *Energy and Fuels*, Vol. 13, pp. 1246-1251, 1999.

4. M. D. Vangsness, S. Zabarnick, N. Widmor, and J. S. Ervin, "Jet Fuel Crystallization at Low Temperatures," PREPRINT, Division of Petroleum Chemistry, American Chemical Society, Vol. 45, pp. 534-537, 2000.

5. D. L. Atkins, J. S. Ervin, M. Vangsness, and C. Obringer, "Flow Visualization of the Freezing of Jet Fuel," Proceedings of the 7th International Conference on Stability and Handling of Liquid Fuels, Graz, Austria, Vol. 2, pp. 841-856, 2001.

6. S. Zabarnick, N. Widmor, J. S. Ervin, and C. Obringer, "Studies of Jet Fuel Freezing and Cold Flow Improving Additives by Differential Scanning Calorimetry," Proceedings of the 7th International Conference on Stability and Handling of Liquid Fuels, Graz, Austria, Vol. 2, pp. 719-730, 2001.

7. S. Zabarnick and N. Widmor, "Studies of Jet Fuel Freezing by Differential Scanning Calorimetry," Energy and Fuels, Vol. 15, pp. 1447-1453, 2001.

8. J. S. Ervin, N. Widmor, S. Zabarnick, and M. Vangsness, "Studies of Jet Fuel Freezing by Differential Scanning Calorimetry and Cold-Stage Microscopy," Transactions of ASME, *Journal of Engineering for Gas Turbines and Power*, Vol. 125, pp. 34-39, 2003.

9. D. L. Atkins and J. S. Ervin, "Flow Visualization of the Freezing of Aviation Fuel," *Energy and Fuels*, Vol. 15, pp. 1233-1240, 2001.

10. S. Zabarnick, and N. Widmor, "Studies of Urea Treatment on the Low Temperature Properties of Jet Fuel," *Energy and Fuels*, Vol. 16, pp. 1565-1570, 2002.

11. N. Widmor, J. S. Ervin, and S. Zabarnick, "Prediction of Freeze Point Temperature of Jet Fuel Using a Thermodynamic Model," *Prepr.-Am. Chem. Soc., Div Pet. Chem.,* Vol. 47, pp. 239-242, 2002.

12. S. Zabarnick, and M. Vangsness, "Properties of Jet Fuels At Low Temperature and the Effect of Additives," *Prepr.-Am. Chem. Soc., Div Pet. Chem.,* Vol. 47, pp. 243-246, 2002.

13. C.A. Obringer, J.S. Ervin, S. Zabarnick, T.F. Williams, M.D. Vangsness, L.M. Shafer, G.L. Dieterle, and K.E. Binns, "Development of Low Temperature Additives for Use in Jet Fuel,"

Proceedings of the 8th International Conference on Stability and Handling of Liquid Fuels, Steamboat Springs, CO, 2003.

14. J. S. Ervin, N. Widmor, S. Zabarnick, and M. Vangsness, "Studies of Jet Fuel Freezing by Differential Scanning Calorimetry and Cold-Stage Microscopy," *Transactions of ASME, Journal of Engineering for Gas Turbines and Power*, Vol. 125, pp. 34-39, 2003.

15. J.S. Ervin, D.L. Atkins, and A. Saxena, "Computational Model of the Freezing of Jet Fuel," Proceedings of the 8th International Conference on Stability and Handling of Liquid Fuels, Steamboat Springs, CO, 2003.

16. S. Zabarnick, M. Laber, J. Ervin, and R. Assudani, "Operation of Aircraft Fuel Systems at Low Temperatures," Proceedings of the 8th International Conference on Stability and Handling of Liquid Fuels, Steamboat Springs, CO, 2003.

17. N. Widmor, J.S. Ervin and S. Zabarnick, "Calculations of Binary Interaction Energies for Solid-Liquid Phase Equilibria Calculations Involving Jet Fuel," *Prepr.-Am. Chem. Soc., Div Pet. Chem.*, Vol. 49, pp. 489-492, 2004.

18. M.D. Vangsness, L. Shafer, J.S. Ervin and S. Zabarnick, "Low-Temperature Properties of Jet Fuel," *Prepr.-Am. Chem. Soc., Div Pet. Chem.*, Vol. 49, pp. 498-501, 2004.

19. R. Assudani, J.S. Ervin and S. Zabarnick, "Computational Fluid Dynamic Simulations of Jet Fuel Flow Near the Freeze Point Temperature," *Prepr.-Am. Chem. Soc., Div Pet. Chem.*, Vol. 49, pp. 502-505, 2004.

20. L.M. Shafer, J.S. Ervin and S. Zabarnick, "Effects of Low-Temperature Additives on Phase Compositions of Jet Fuel," *Prepr.-Am. Chem. Soc., Div Pet. Chem.*, Vol. 49, pp. 506-509, 2004.

21. T.W. Selby and M. Vangsness, "Studies of Flow and Gelation Response of Jet Fuels at Critical Low Temperatures," presented at the International Condition Monitoring Conference – Joint Oil Analysis Program, 2004.

22. D. Atkins, J.S. Ervin, and L. Shafer, "Experimental Studies of Jet Fuel Viscosity at Low Temperatures, Using a Rotational Viscometer and an Optical Cell," *Energy & Fuels*, Vol. 19, pp. 1935-1947, 2005.

23. D.L. Atkins, J.S. Ervin, and A. Saxena, "Computational Model of the Freezing of Jet Fuel," *AIAA J. Propulsion and Power*, Vol. 21, pp. 356-367, March-April 2005.

24. R. Assudani, J.S. Ervin, S. Zabarnick, and L. Shafer, "Experimental and Computational Studies of Jet Fuel Flow Near the Freeze Point," *AIAA J. Propulsion and Power*, Vol. 22, pp. 534-541, 2006.

25. R. Assudani, J.S. Ervin, and L. Riehl, "Experiments and Simulations of the Freezing of Jet Fuel in Forced Flow," *AIAA J. Propulsion and Power*, Vol. 23, pp. 1123-1133, 2007.

26. J.S. Ervin, S. Zabarnick, L.J. Shafer, M.D. Vangsness, K.E. Binns, T.F. Williams, G.L. Dieterle, D.G. Davis, R.J. Strong, M.J. DeWitt, D.K. Phelps, C. Obringer, D.K. Atkins, and W.E. Harrison, III, "Development of an Advanced Jet Fuel with Improved Low Temperature Flow Performance – The JP-8+100LT Program," U.S. Air Force Research Laboratory Report, AFRL-RZ-WP-TR-2011-2054, 2011.

27. S. Zabarnick and J.S. Ervin, "The Effects of Operating Jet Fuels Below the Specification Freeze Point Temperature Limit," DOT/FAA/AR-09/50, 2010.

28. G. Latini, R.C. Grifoni, and G. Passerini, "Transport Properties of Organic Liquids," WIT Press, Billerica, MA, 2006.

29. D.S. Viswanath, T.K. Ghosh, D.H.L. Prasad, N.V.K. Dutt, and K.Y. Rani, "Viscosity of Liquids : Theory, Estimation, Experiment, and Data," Springer Netherlands, 2007.

30. "Interlaboratory Study for Freezing Point of Aviation Fuels Including Contaminated Jet Fuels," RR D02-1536, Jan 2003.

Appendix

Table A1. Compiled Viscosity and Density Data for Fuels Studied

POSF	Fuel Type	ASTM D5972	Scanning Brookfield Viscometer (ASTM D5133)			Capillary Viscometer (ASTM D445)		Density (g/mL)		
		T_{fp} (°C)	T_{knee} (°C)	ν_{knee} (cSt)	ν_{fp} (cSt)	ν_{-40C} (cSt)	ν_{-20C} (cSt)	-40°C	-20°C	15°C
2827	Jet A	-50.0	-54.1	14.8	11.4	8.2	4.1	0.842		0.804
2926	Jet A	-43.3	-47.5	16.0	12.7	10.9	5.4	0.849	0.839	0.807
3084	Jet A	-46.0	-48.9	17.5	14.2	10.8	5.0	0.846		0.808
3166	Jet A	-44.8	-47.5	16.3	14.0	11.3	5.3	0.848		0.809
3219	Jet A	-47.1	-51.5	20.8	15.6	10.7	5.2	0.848		0.811
3602	Jet A	-53.9	-57.2	28.4	23.5	10.6	5.0	0.859		0.820
3633	Jet A	-55.6	-58.8	19.6	15.7	7.7	4.0	0.843		0.806
3638	Jet A	-53.1	-55.4	17.1	15.0	7.8	3.9	0.835		0.793
3658	Jet A	-55.7				17.1	6.7	0.876		0.837
3683	Jet A	-42.2	-45.7	16.9	13.5	12	5.4	0.852	0.838	0.813
3686	Jet A	-43.6	-46.9	17.9	15.2	12.2	5.6	0.861	0.848	0.823
3688	Jet A	-42.5	-46.25	15.6	12.5	10.2	4.8	0.837	0.824	0.800
3694	Jet A	-50.0	-54.2	19.2	15.6	9.6	4.5	0.845		0.807
2747	Jet A-1	-60.4	-63.6	28.6	22.9	8.2	4.1	0.846		0.808
4877	Jet A-1	-52.3	-54.8	17.6	16.1	8.4	4.2	0.836	0.821	0.797
3773	JP-8	-49.7	-54.3	15.9	12.2	8.1	4.1	0.834	0.823	0.798
3804	JP-8	-48.8	-52.5	15.7	12.8	8.3	4.2	0.836	0.823	0.798
4177	JP-8	-57.7	-60.2	32.5	28.1	10.2	4.9	0.853		0.814
4336	JP-8	-48.1	-51.8	28.6	21.8	13.7	5.9	0.860		0.823
4339	JP-8	-50.6	-52.9	17.7	15.0	8.8	4.3	0.833		0.795
4351	JP-8	-52.5	-56.7	35.1	26.6	13.0	5.9	0.864		0.826
4751	JP-8	-50.2	-53.1	20.4	16.4	9.9	4.9	0.843	0.829	0.804
4908	JP-8	-50.4	-54.1	25.4	20.6	11.1	5.1	0.845		0.808
4911	JP-8	-52.0	-54.6	23.7	19.4	9.4	4.8	0.845		0.807
5699	JP-8	-50.4	-54.1	16.7	14.0	8.0	4.0	0.832		0.795
6169	JP-8	-49.8	-53.9	16.6	13.2	8.7	4.2	0.836	0.821	0.798
4909	F-T SPK	-51.3	-53.4	18.2	16.2	9.5	4.9	0.793	0.779	0.756
4913	F-T SPK/JP-8 Blend	-50.9	-53.4	19.8	16.8	9.7	4.7	0.818	0.804	0.780
5018	F-T SPK	-49.4	-54.8	20.1	14.5	9.6	5.0	0.794	0.779	0.755
5172	F-T SPK	-53.8	-63.7	12.5	7.9	4.4	2.6	0.777	0.762	0.737
5225	F-T SPK/JP-8 Blend	-58.7	-64.2	20.7	14.0	6.3	3.5	0.820	0.800	0.771
5698	F-T SPK	-50.2	-54.7	23.3	16.7	10.9	5.0	0.798	0.786	0.763
6399	HRJ/JP-8 Blend	-54.8	-59.7	27.5	20.7	9.6	4.6	0.813	0.802	0.778
6406	HRJ/JP-8 Blend	-54.5	-59.7	28.3	20.0	10.1	5.0	0.820	0.804	0.781
6866	Biojet	-61.9	-66.9	29.1	22.7	7.6	3.8	0.834	0.818	0.794
7060	ATJ/JP-8	-57.0	-62.1	29.5	21.5	9.5	5.1	0.812	0.804	0.783
7449	Biojet	-58.2	-65.7	38.4	22.6	9.2	4.5	0.835	0.814	0.791
7718	F-T SPK/JP-8 Blend	-58.0	-61.6				3.9			0.779
6308	HRJ-Tallow	-61.9				10.6	5.3	0.796	0.782	0.758
5642	F-T SPK	<-65				7.0	3.6	0.799	0.781	0.762
6882	ATJ	<-65				9.7	4.9	0.798	0.785	0.762
7629	F-T SPK	<-60					3.8			0.760

Table A2. Normal Alkane Content of 26 Petroleum Fuels Studied

POSF	Fuel Type	n-Alkane Distribution by Carbon Number (wt%)													Total n–Alkanes (wt%)	Sum of n-Alkane Ranges (wt%)		
		nC7	nC8	nC9	nC10	nC11	nC12	nC13	nC14	nC15	nC16	nC17	nC18	nC19		nC_7 - nC_{10}	nC_{11} - nC_{13}	nC_{14} - nC_{19}
2827	Jet A	0.10	0.37	1.88	3.13	2.71	2.18	1.71	1.18	0.56	0.14	0.034	0.007	0.002	14.0	5.5	6.6	1.9
2926	Jet A	0.065	0.33	1.35	3.22	3.78	2.85	2.45	1.92	1.29	0.50	0.074	0.005	<0.001	17.8	5.0	9.1	3.8
3084	Jet A	0.050	0.26	1.24	2.85	3.71	3.22	2.66	1.86	0.99	0.37	0.12	0.035	0.014	17.4	4.4	9.6	3.4
3166	Jet A	0.082	0.33	1.27	2.71	4.24	4.01	3.58	2.79	1.55	0.45	0.13	0.031	0.011	21.2	4.4	11.8	5.0
3219	Jet A	0.047	0.23	0.78	2.93	4.17	3.54	2.79	2.00	1.23	0.49	0.069	0.010	0.006	18.3	4.0	10.5	3.8
3602	Jet A	0.028	0.40	0.98	1.53	3.90	3.37	2.54	1.47	0.61	0.16	0.05	0.012	0.005	15.1	2.9	9.8	2.3
3633	Jet A	<0.002	0.03	2.41	4.00	4.53	4.25	2.88	0.99	0.25	0.06	0.02	0.008	0.005	19.4	6.4	11.7	1.3
3638	Jet A	0.099	0.47	1.33	5.12	6.91	4.69	2.87	0.80	0.15	0.025	0.006	0.001	0.001	22.5	7.0	14.5	1.0
3658	Jet A	0.004	0.020	0.088	0.68	1.66	1.26	0.88	0.71	0.39	0.22	0.11	0.040	0.017	6.1	0.79	3.8	1.5
3683	Jet A	0.21	0.53	2.02	5.10	5.81	5.23	4.61	3.69	2.47	1.35	0.52	0.14	0.037	31.7	7.9	15.6	8.2
3686	Jet A	<0.002	0.27	1.24	1.87	2.31	2.28	2.05	1.71	1.26	0.73	0.33	0.100	0.044	14.2	3.4	6.6	4.2
3688	Jet A	<0.002	0.51	1.25	3.15	4.28	3.65	2.98	2.25	1.56	0.76	0.24	0.036	0.009	20.7	4.9	10.9	4.9
3694	Jet A	0.069	0.45	1.69	3.04	3.77	3.24	2.91	1.85	0.84	0.25	0.09	0.027	0.012	18.2	5.3	9.9	3.1
2747	Jet A-1	0.002	0.003	0.074	3.51	6.41	3.39	0.99	0.25	0.059	0.019	0.009	0.004	0.002	14.7	3.6	10.8	0.34
4877	Jet A-1	0.028	0.15	1.17	4.30	7.69	6.09	3.41	1.20	0.33	0.078	0.023	0.007	0.003	24.5	5.7	17.2	1.6
3773	JP-8	0.12	0.41	2.42	3.78	3.85	3.16	2.48	1.75	0.88	0.26	0.054	0.008	0.003	19.2	6.7	9.5	3.0
3804	JP-8	0.13	0.44	2.22	4.72	5.10	4.28	3.56	2.30	0.82	0.15	0.03	0.006	0.002	23.8	7.5	12.9	3.3
4177	JP-8	0.077	0.23	0.64	1.74	2.89	2.74	2.04	0.97	0.39	0.14	0.07	0.031	0.016	12.0	2.7	7.7	1.6
4336	JP-8	0.017	0.14	0.65	1.61	3.15	3.50	2.82	2.11	0.83	0.061	0.017	0.011	0.009	14.9	2.4	9.5	3.0
4339	JP-8	0.12	0.50	1.58	4.33	5.70	4.95	3.56	1.85	0.63	0.14	0.036	0.014	0.009	23.4	6.5	14.2	2.7
4351	JP-8	0.002	0.060	0.039	1.14	2.07	2.02	1.71	1.33	0.49	0.064	0.023	0.010	0.006	9.0	1.2	5.8	1.9
4751	JP-8	0.10	0.34	1.21	3.48	4.24	3.71	2.84	1.79	0.87	0.27	0.089	0.024	0.008	19.0	5.1	10.8	3.1
4908	JP-8	0.029	0.10	0.39	2.13	5.21	4.69	3.49	1.77	0.57	0.12	0.035	0.009	0.002	18.5	2.6	13.4	2.5
4911	JP-8	0.12	0.48	1.47	2.33	2.66	2.30	1.93	1.40	0.77	0.32	0.16	0.072	0.025	14.0	4.4	6.9	2.7
5699	JP-8	0.11	0.47	1.82	5.16	4.47	3.58	2.74	1.60	0.55	0.13	0.039	0.013	0.006	20.7	7.6	10.8	2.3
6169	JP-8	0.13	0.50	1.85	4.32	4.70	4.14	3.01	1.75	0.78	0.24	0.081	0.023	0.008	21.5	6.8	11.8	2.9
	Average	0.075	0.31	1.27	3.15	4.23	3.55	2.67	1.67	0.81	0.29	0.095	0.026	0.010	18.1	4.8	10.4	2.9
	Max	0.21	0.53	2.42	5.16	7.69	6.09	4.61	3.69	2.47	1.35	0.52	0.14	0.044	31.7	7.9	17.2	8.2
	Min	<0.002	0.003	0.039	0.68	1.66	1.26	0.88	0.25	0.059	0.019	0.006	0.001	<0.001	6.1	0.79	3.8	0.34